Quaternary Research 86 (2016) 271–286

Contents lists available at ScienceDirect

Quaternary Research

journal homepage: http://www.journals.elsevier.com/quaternary-research

The Carolina Sandhills: Quaternary eolian sand sheets and dunes along the updip margin of the Atlantic Coastal Plain province, southeastern United States

Christopher S. Swezey [a, *], Bradley A. Fitzwater [b], G. Richard Whittecar [b], Shannon A. Mahan [c], Christopher P. Garrity [d], Wilma B. Alemán González [a], Kerby M. Dobbs [e]

[a] U.S. Geological Survey, 12201 Sunrise Valley Drive, MS 926A, Reston, VA 20192, USA
[b] Old Dominion University, Dept. of Ocean, Earth, and Atmospheric Sciences, Norfolk, VA 23529, USA
[c] U.S. Geological Survey, Box 25046 Denver Federal Center, MS 974, Denver, CO 80225, USA
[d] U.S. Geological Survey, 12201 Sunrise Valley Drive, MS 956, Reston, VA 20192, USA
[e] Maser Consulting, 2000 Midlantic Drive, MT. Laurel, NJ 08054, USA

ARTICLE INFO

Article history:
Received 8 March 2016
Available online 20 October 2016

Keywords:
Eolian
Pinehurst Formation
Quaternary
South Carolina

ABSTRACT

The Carolina Sandhills is a physiographic region of the Atlantic Coastal Plain province in the southeastern United States. In Chesterfield County (South Carolina), the surficial sand of this region is the Pinehurst Formation, which is interpreted as eolian sand derived from the underlying Cretaceous Middendorf Formation. This sand has yielded three clusters of optically stimulated luminescence ages: (1) 75 to 37 thousand years ago (ka), coincident with growth of the Laurentide Ice Sheet; (2) 28 to 18 ka, coincident with the last glacial maximum (LGM); and (3) 12 to 6 ka, mostly coincident with the Younger Dryas through final collapse of the Laurentide Ice Sheet. Relict dune morphologies are consistent with winds from the west or northwest, coincident with modern and inferred LGM January wind directions. Sand sheets are more common than dunes because of effects of coarse grain size (mean range: 0.35–0.59 mm) and vegetation. The coarse grain size would have required LGM wind velocities of at least 4–6 m/sec, accounting for effects of colder air temperatures on eolian sand transport. The eolian interpretation of the Carolina Sandhills is consistent with other evidence for eolian activity in the southeastern United States during the last glaciation.

Introduction

The Carolina Sandhills is a 15–60 km wide physiographic region that extends from the western border of Georgia (GA) across South Carolina (SC) to central North Carolina (NC) along the updip (north and west) margin of the Atlantic Coastal Plain province in the southeastern United States (Fig. 1). This region is characterized by abundant unconsolidated sand that has been recognized for a long time (e.g., McGee, 1890, 1891; Holmes, 1893), although previous studies of this region are surprisingly few and previous interpretations of the sand have been quite speculative. Cooke (1936), for example, suggested that eolian processes played a role in shaping the topography of the area (which he called the “Congaree Sand Hills”), and he noted that the area of the sand hills corresponds to the area where the Cretaceous Tuscaloosa Formation [Middendorf Formation] is exposed. Other previous studies in South Carolina have referred to the sand hills as being of post-Eocene age, and speculations on depositional environment have ranged from eolian to fluvial to marine (Johnson, 1961; Otwell et al., 1966; Ridgeway et al., 1966; Kite, 1987; Nystrom and Kite, 1988). Nystrom et al. (1991) stated that the sand hills are widespread deposits of sand dispersed discontinuously across the upper coastal plain from northern Aiken County (SC) northeastward to the SC-NC border, and that these deposits are the southwestern continuation of the Pinehurst Formation of North Carolina, as named by Conley (1962) and redefined by Bartlett (1967). Nystrom et al. (1991) interpreted the sand as eolian dunes, sand sheets, and interdune deposits of Late Miocene age. However, a subsequent detailed study

* Corresponding author.
E-mail address: cswezey@usgs.gov (C.S. Swezey).

http://dx.doi.org/10.1016/j.yqres.2016.08.007
0033-5894/Published by Elsevier Inc. on behalf of University of Washington.

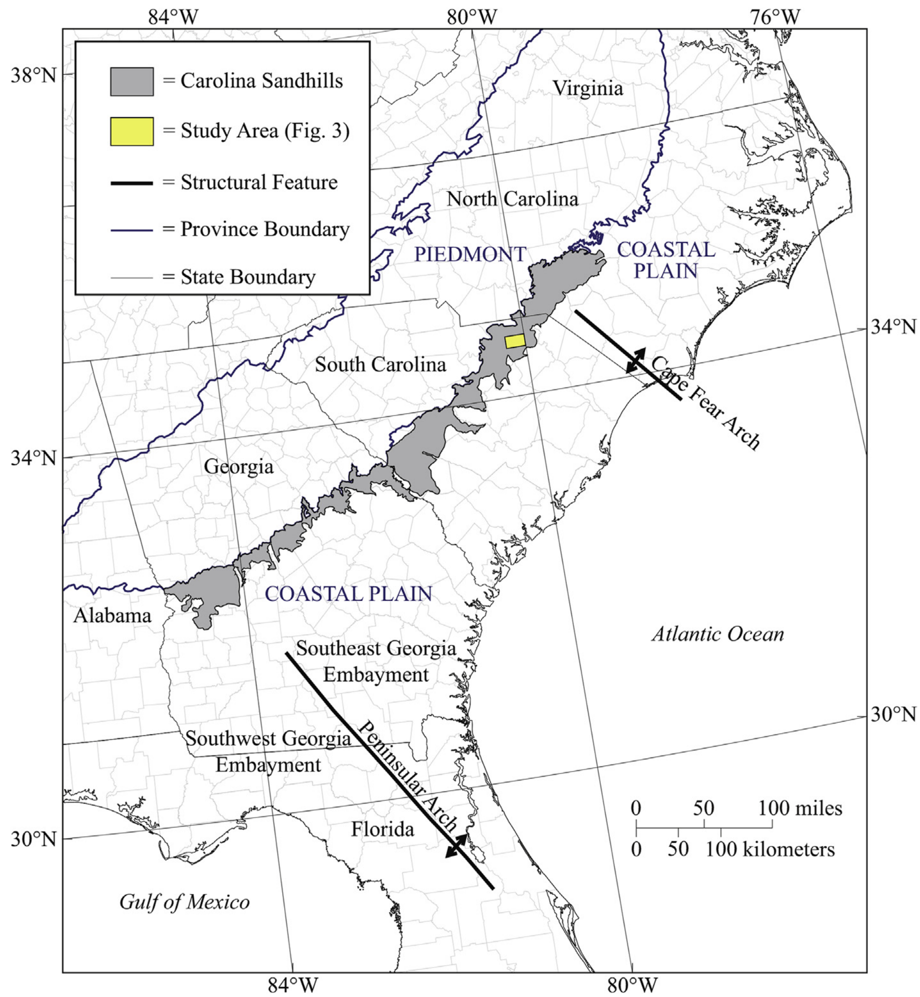

Figure 1. Location of the Carolina Sandhills in the southeastern United States (from Griffith et al., 2001, 2002). Locations of the Cape Fear Arch and Peninsular Arch are from LeGrand (1961).

by Leigh (1998) in Chesterfield County (SC) interpreted the sand hills as eolian, fluvial, and marine sediments of Pliocene to Holocene age. Since the work by Leigh (1998), few studies have been published on the Pinehurst Formation, but the debate on both the origin and the age of the sand hills has continued vigorously among geologists working in the area.

This paper presents new data on the Carolina Sandhills region in Chesterfield County, South Carolina (Fig. 2). These new data situate the sand hills in a robust stratigraphic and chronologic framework, and they support interpretations of the sand as eolian sand sheets and dunes that were active episodically circa (ca.) 75 to 6 thousand years ago (ka). Furthermore, the eolian nature of the sand permits the reconstruction of several paleoclimate variables, and comparison with previously published data suggests that eolian activity was widespread during this time in the southeastern United States.

Study area

The study area is located within the Carolina Sandhills region in Chesterfield County, South Carolina (Fig. 2). In this county, sand hills and sand sheets occur on a relatively high plateau of Cretaceous strata, bounded to the west by Paleozoic schist of the Piedmont Province and bounded to the east by the east-facing Orangeburg Scarp (Swift and Heron, 1969). The Orangeburg Scarp (Fig. 2) is interpreted as a shoreline formed by wave erosion during a middle Pliocene time of high sea level (Dowsett and Cronin, 1990). East of the scarp, the coastal plain exhibits relatively low-relief and is dominated by oval depressions (Carolina Bays) that are thought to have formed by eolian deflation (e.g., Thom, 1970; Kaczorowski, 1977; Ivester et al., 2002, 2003; Moore et al., 2014, 2016).

Most of the information presented in this paper is based on detailed geologic mapping of the Middendorf and Patrick quadrangles within the Carolina Sandhills region of Chesterfield County. These two adjacent quadrangles (Fig. 2) contain the following three major geologic units:

(1) a 60- to 150-m-thick unit of weakly consolidated sandstone, sand, and mud that extends throughout the entire study area and is mapped as the Cretaceous Middendorf Formation. Cores drilled in the study area show that this unit rests on an unconformity above Paleozoic schist;
(2) a 0.3- to 10-m-thick unit of unconsolidated sand that overlies an unconformity on the Middendorf Formation throughout most of the study area. This unit forms the "sandhills" of the region, and is mapped as the Quaternary Pinehurst Formation;
(3) a <3-m-thick unit of sand, sandy mud, and mud that is present adjacent to some of the modern drainages and is mapped as Quaternary fluvial terrace deposits.

https://doi.org/10.1016/j.yqres.2016.08.007 Published online by Cambridge University Press

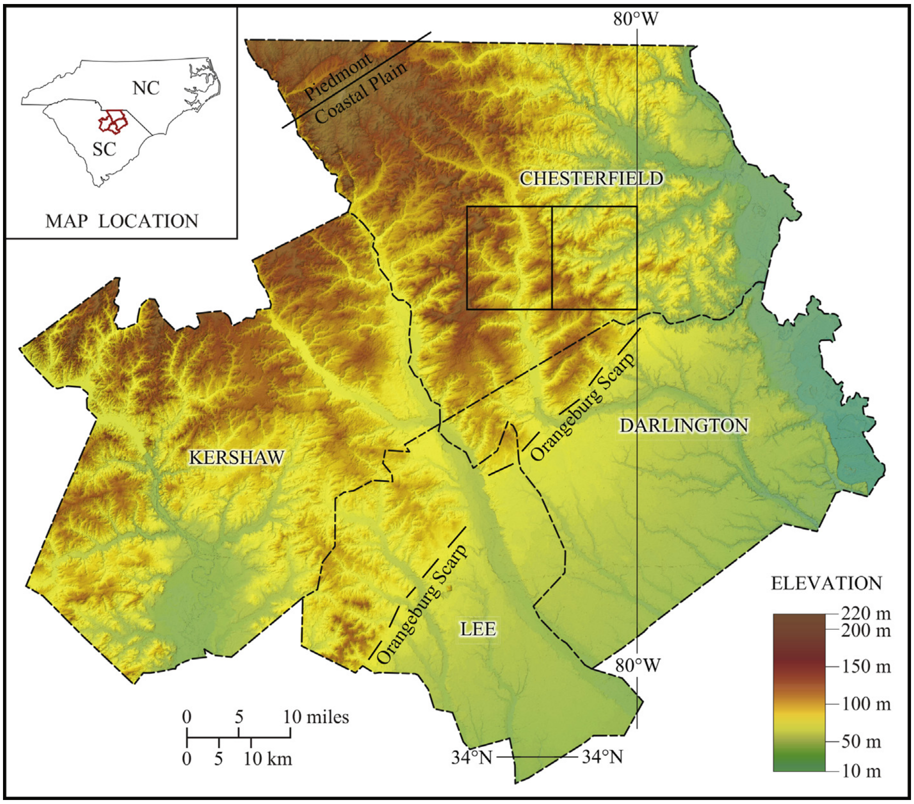

Figure 2. Shaded relief map of Kershaw, Chesterfield, Lee, and Darlington Counties, South Carolina. Two-meter elevation data are derived from LiDAR point cloud data (South Carolina LiDAR Consortium, 2007, LiDAR and related data products, last accessed July 19, 2015 at http://www.dnr.sc.gov/GIS/lidar.html). Black rectangles show the locations of the Middendorf quadrangle (on the west) and the Patrick quadrangle (on the east), which are shown in greater detail in Fig. 3.

Imagery of the Middendorf and Patrick quadrangles derived from LiDAR point cloud data reveals relatively flat topographically high areas incised by creeks and streams (Fig. 3). In the Middendorf quadrangle most of the creeks and streams are south-flowing drainages associated with Big Black Creek, whereas in the Patrick quadrangle most of the creeks and streams are east-flowing drainages (e.g., Juniper Creek). A prominent north-trending escarpment characterized by arcuate embayments at stream headwaters forms the drainage divide between the two major fluvial systems (Fig. 3).

Under prevailing climate conditions, the Carolina Sandhills region is stabilized by xeric sand community vegetation dominated by pine trees (Christensen, 2000; Earley, 2004; Sorrie, 2011). In Chesterfield County, the overstory vegetation is primarily longleaf pine (*Pinus palustris*) and a groundcover of wiregrass (*Aristida stricta*), which compose an ecosystem that is dependent upon frequent ground fires (Earley, 2004). Other trees within this portion of the Carolina Sandhills include turkey oak (*Quercus laevis*), dwarf post oak (*Quercus margarettae*), and blackjack oak (*Quercus marilandica*). In addition, pond cypress (*Taxodium ascendens*) and sweetgum (*Liquidambar styraciflua*) are present along some creeks.

Modern climate

The modern climate of Chesterfield County is humid and mesothermal with little or no water deficiency during any season (climate classification of Thornthwaite, 1931, 1948). The mean temperature varies from approximately 7°C in January to 27°C in July (Fig. 4). Precipitation occurs throughout the year, mean annual precipitation is approximately 119 cm, and average annual potential evapotranspiration is approximately 90 cm (Fig. 5). These values yield a ratio of annual precipitation to potential evapotranspiration (P:PE) of 1.32.

The directions of surface winds in the southeastern United States vary seasonally (Fig. 4) and are mostly associated with cyclones and anticyclones, which are governed primarily by the following three variables: (1) the westerlies; (2) the polar front jet stream; and (3) the Bermuda High. During the winter (when the latitudinal thermal gradient is greater), the polar front jet stream moves to lower latitudes, the westerlies and the polar front jet stream are stronger and exhibit predominantly zonal flow (flow relatively parallel to the lines of latitude), and the Bermuda High is weak (Sahsamanoglou, 1990; Harman, 1991; Davis et al., 1997). As a result, surface winds over South Carolina blow predominantly from the west and west-northwest, and most precipitation in South Carolina is frontal in association with the polar front jet stream where cold and dry continental polar air from Canada is in contact with warm and humid maritime air from the Gulf of Mexico (Court, 1974; Soulé, 1998; Katz et al., 2003). In contrast, during the summer the polar front jet stream moves to higher latitudes, the westerlies and the polar front jet stream are weaker and exhibit predominantly meridional flow (flow with large meanders and a greater north-south trajectory), and the Bermuda High is strong (Sahsamanoglou, 1990; Harman, 1991; Davis et al., 1997). As a result, surface winds over South Carolina change direction and blow from the south via the Bermuda High, bringing increased moisture from the Atlantic Ocean to South Carolina (Court, 1974; Soulé, 1998; Katz et al., 2003). Most precipitation during the summer is associated with convection rather than fronts. In addition, tropical cyclones (including hurricanes) occur most frequently during June through October, and they account for approximately 10–15% of the total precipitation in the Carolina

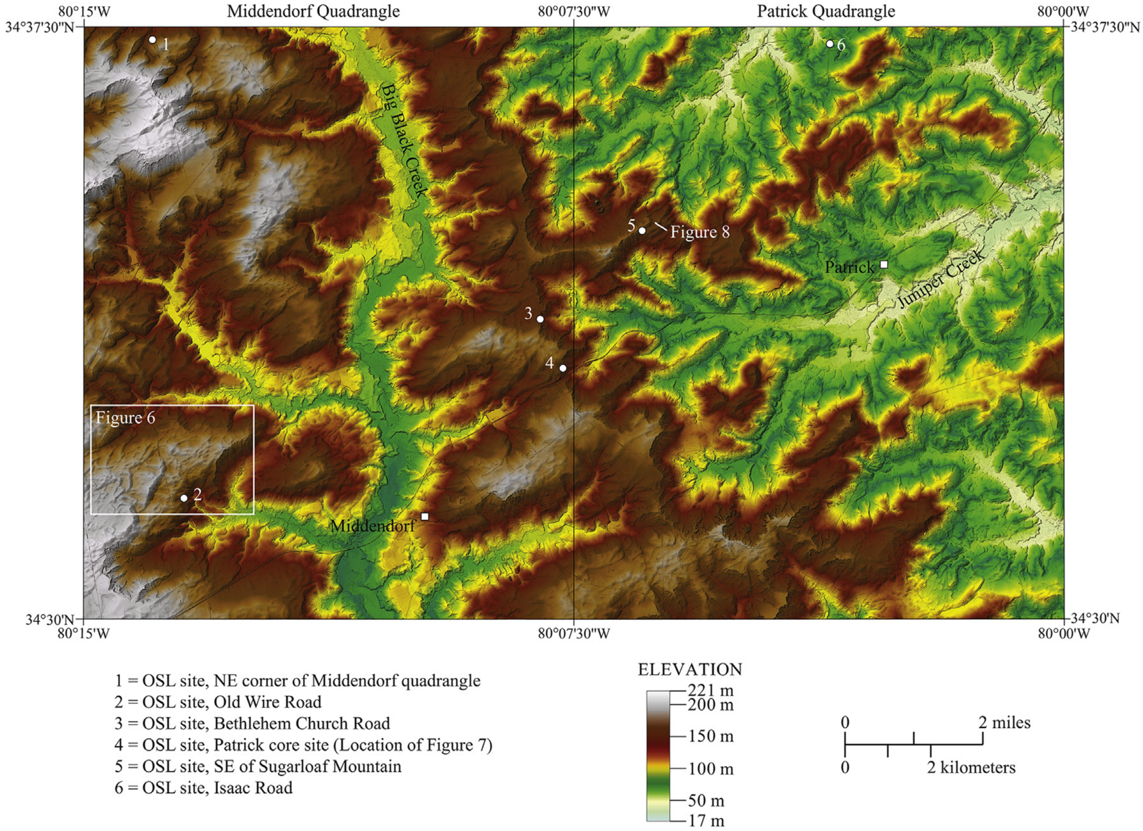

Figure 3. Shaded relief map of the Middendorf and Patrick quadrangles, Chesterfield County, South Carolina. Two-meter elevation data are derived from LiDAR point cloud data (South Carolina LiDAR Consortium, 2007, LiDAR and related data products, last accessed July 19, 2015 at http://www.dnr.sc.gov/GIS/lidar.html). White circles with numbers denote OSL sites, and white squares denote small towns.

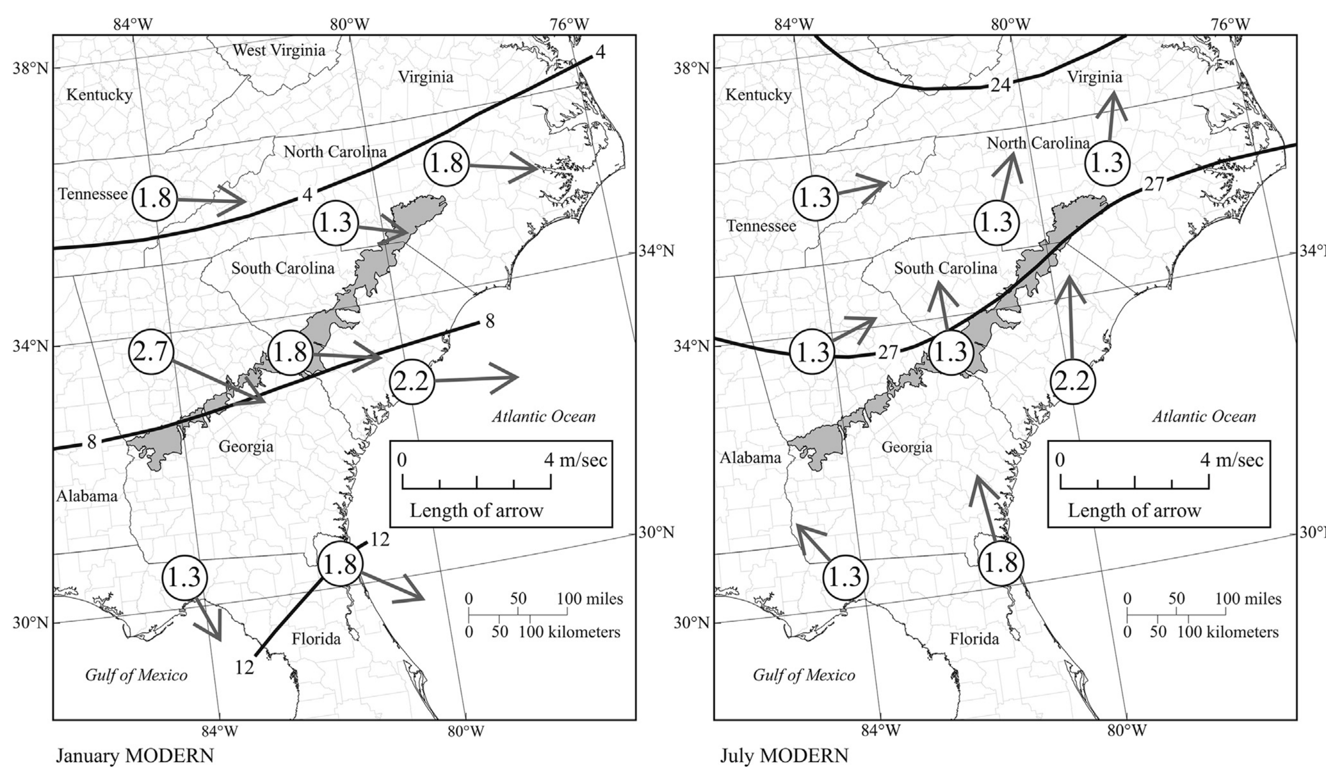

Figure 4. Data from January (left image) and July (right image) of modern mean temperature in degrees Celsius (Webb et al., 1993), and mean resultant velocity and direction of surface winds based on hourly observations from 1951 through 1960 (data from Baldwin, 1975). The wind velocity in meters per second (m/s) is written inside each circle, and is also denoted by the length of the gray arrows. The mean resultant wind is the vectorial average of all wind velocities and wind directions at a given place during the specified months for 1951 to 1960.

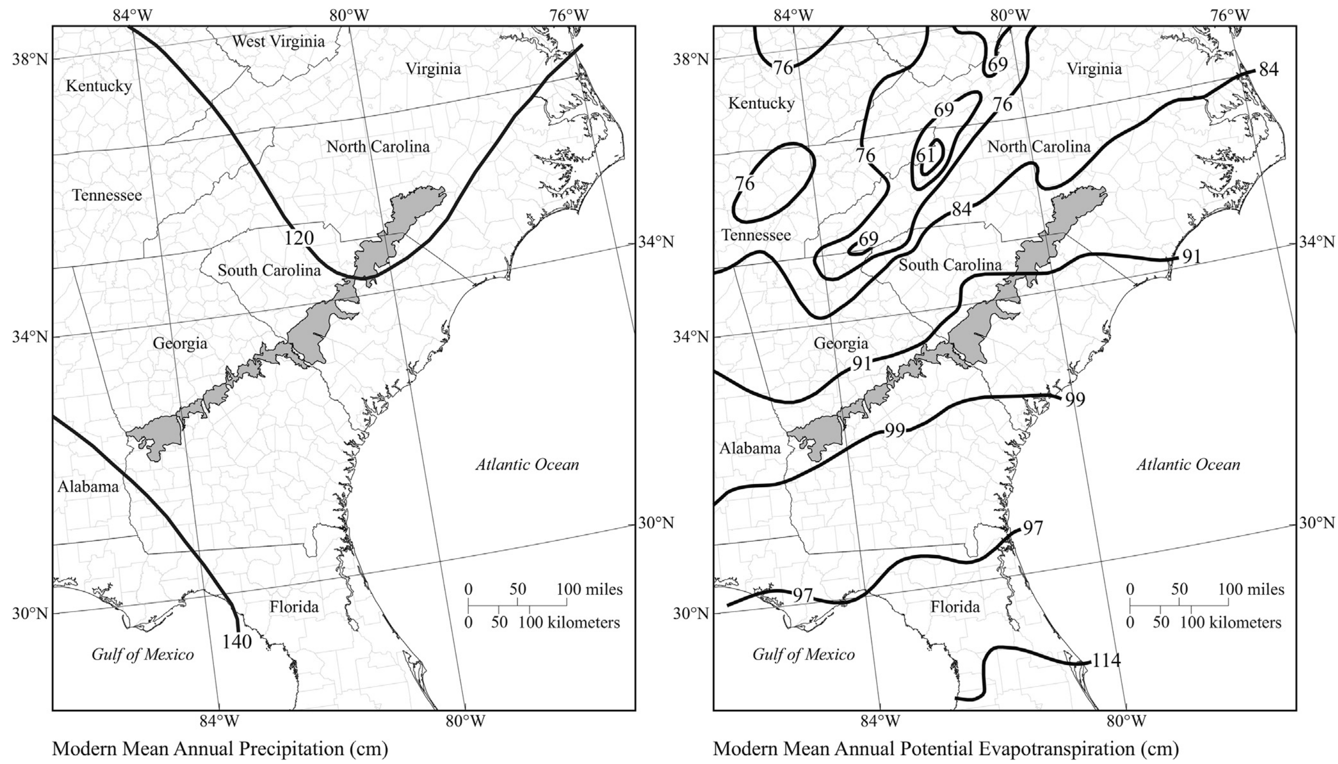

Figure 5. Mean annual precipitation in centimeters (Webb et al., 1993) and mean annual evapotranspiration in centimeters (Thornthwaite, 1948).

portion of the coastal plain (Court, 1974; Knight and Davis, 2007). During some summers, however, the western sector of the Bermuda High moves westward of its mean position to an inland location over the southeastern United States, and moisture flux from the Gulf of Mexico to the southeastern United States is reduced (Stahle and Cleaveland, 1992).

The mean resultant velocity of surface winds in South Carolina is <3 m/sec during any given month (Fig. 4), but there is some variability ("gustiness") around the mean. Detailed hourly data from the Metropolitan Airport at the city of Columbia (Carolina Sandhills region, approximately 100 km southwest of the Middendorf quadrangle) indicate that wind velocities of 6 m/sec or greater occurred approximately 8% of the time per whole year during the interval of 1981–2010 (www.ncdc.noaa.gov; accessed 18 August 2016). Using a 6 m/sec threshold wind velocity for eolian sand mobilization, the 1981–2010 data yield a drift potential of 75 vector units (VU) and a resultant drift direction for eolian sediment of 97° (slightly south of east). For reference, a drift potential of 75 VU is in the "low-energy wind environment" category of Fryberger and Dean (1979).

Methods

Sediment grain sizes were described using terminology of Wentworth (1922) and Folk (1954, 1980). Selected samples were subjected to size analysis using a Malvern Mastersizer 2000 laser diffractometer (Fitzwater, 2016). Other samples were subjected to sieving analysis using mesh sizes at 0.5 phi (ϕ) increments, and sieving times of at least 15 min per sample (following Folk and Ward, 1957; Folk, 1966). For sieved samples, sediment sorting values were calculated from cumulative percent curves using the sorting formula of Folk and Ward (1957), and sediment textural maturity was described using terminology of Folk (1951, 1954, 1956). A binocular microscope was used to determine both sediment grain shape (using sphericity and roundness terminology of Powers, 1953) and sediment grain composition. The determination of sediment composition was done visually via point counting (following procedures of van der Plas and Tobi, 1965; Folk et al., 1970; Folk, 1980).

Ground-penetrating radar (GPR) data were collected with a Geophysical Survey Systems, Inc. (GSSI) towed-array data acquisition system using a Subsurface Interface Radar (SIR-3000) and 200 megahertz (MHz) antenna outfitted with an integrated survey wheel that was calibrated in the field. Post-processing of GPR data was conducted using RADAN (version 7) processing software. Specific GPR setup parameters and post-processing filter constraints are described in Fitzwater (2016).

The ages of some sediment samples were determined using optically stimulated luminescence (OSL) techniques at the U.S. Geological Survey (USGS) luminescence laboratory in Denver, Colorado (Tables 1 and 2). Samples were collected in 0.8-m-long opaque polyvinyl chloride (PVC) tubes that were hammered into the sediment, in most instances at the base of pits dug into sand hills and terraces. The tubes were then extracted and capped to prevent light exposure. Following standard laboratory procedures (Wintle and Murray, 2006; Mahan et al., 2007), the samples were treated with acids to remove carbonate and organic matter, and then sieved to extract fine-grained sand (250–180 μm). Quartz sand was separated from other grains by heavy liquid immersion, and quartz grains were etched by hydrofluoric acid to remove the outermost layer. The purified quartz samples were analyzed using the single-aliquot regeneration technique (Murray and Wintle, 2000, 2003), and a minimum of 20 aliquots were measured for each sample. Dose response tests, preheat plateau tests, and thermal transfer tests were performed to ensure that the sediment was responsive to optical techniques and that proper preheat temperatures were used in producing the equivalent dose (DE) values. The DE values were determined by the single-aliquot regenerative

Table 1
Optically stimulated luminescence (OSL) data from sand of the Pinehurst Formation, Chesterfield County, South Carolina. CDA (Gy/ka) = Cosmic Dose Additions (grays per thousand years) as calculated using the methods of Prescott and Hutton (1994); DEPTH (cm) = sample depth (centimeters below surface); DR (Gy/ka) = total dose rate (grays per thousand years) with cosmic dose additions (grays per thousand years) as calculated using the methods of Prescott and Hutton (1994); ELV (m) = sample site elevation (meters above sea level); K (%) = potassium content (percentage); LAT = latitude; LONG = longitude; SITE # (Fig. 3) = OSL site number shown in Fig. 3; Th (ppm) = thorium content (parts per million); U (ppm) = uranium content (parts per million); USGS ID = U.S. Geological Survey OSL laboratory sample identification code; WATER (%) = field moisture (complete sample saturation percentage in parentheses); YEAR = Year during which sample age was determined.

USGS ID	YEAR	SITE # (Fig. 3)	LAT (North)	LONG (West)	ELV (m)	DPTH (cm)	WATER (%)	K (%)	U (ppm)	Th (ppm)	CDA (Gy/ka)	DR (Gy/ka)
1585	2013	3	34.56355	−80.13365	113	42–47	2 (22)	0.24 ± 0.04	1.57 ± 0.21	5.75 ± 0.52	0.20 ± 0.02	1.10 ± 0.08
1586	2013	3	34.56355	−80.13365	113	65–70	2 (16)	0.23 ± 0.04	1.51 ± 0.20	6.20 ± 0.56	0.19 ± 0.01	1.14 ± 0.08
1588	2013	5	34.58355	−80.10430	125	42	5 (19)	0.24 ± 0.04	1.07 ± 0.24	3.82 ± 0.35	0.20 ± 0.02	0.89 ± 0.39
1589	2013	5	34.58355	−80.10430	125	85	3 (22)	0.25 ± 0.02	1.70 ± 0.11	6.55 ± 0.26	0.19 ± 0.01	2.31 ± 0.87
1642	2013	4	34.55686	−80.12839	119	200	4 (27)	0.21 ± 0.04	1.05 ± 0.18	6.77 ± 0.37	0.16 ± 0.01	0.96 ± 0.05
1643	2013	4	34.55686	−80.12839	119	60	7 (28)	0.24 ± 0.04	1.80 ± 0.23	8.52 ± 0.47	0.19 ± 0.01	1.27 ± 0.06
1715	2014	6	34.62072	−80.05958	76	210	6 (28)	0.22 ± 0.04	1.88 ± 0.24	10.5 ± 0.31	0.16 ± 0.01	1.35 ± 0.04
1716	2014	6	34.62072	−80.05958	76	250	3 (26)	0.12 ± 0.06	1.33 ± 0.33	5.36 ± 0.43	0.15 ± 0.01	0.85 ± 0.07
1717	2014	6	34.62072	−80.05958	76	250	4 (25)	0.17 ± 0.04	1.28 ± 0.28	6.07 ± 0.59	0.15 ± 0.01	0.93 ± 0.08
1718	2014	2	34.52557	−80.22427	122	40	6 (30)	0.35 ± 0.03	0.84 ± 0.21	3.02 ± 0.53	0.21 ± 0.02	0.83 ± 0.10
1719	2014	2	34.52557	−80.22427	122	145	6 (25)	0.14 ± 0.04	1.04 ± 0.23	2.16 ± 0.47	0.17 ± 0.01	0.63 ± 0.10
1720	2014	1	34.62237	−80.23235	125	90	9 (30)	0.25 ± 0.05	1.26 ± 0.21	5.90 ± 0.41	0.19 ± 0.02	0.99 ± 0.05
1721	2014	1	34.62237	−80.23235	125	160	7 (28)	0.40 ± 0.06	2.67 ± 0.27	10.2 ± 0.68	0.17 ± 0.01	1.65 ± 0.09
1722	2014	1	34.62237	−80.23235	125	210	10 (25)	0.43 ± 0.04	2.67 ± 0.28	10.60 ± 0.48	0.16 ± 0.01	1.72 ± 0.07

Table 2
Optically stimulated luminescence (OSL) equivalent dose data and ages from sand of the Pinehurst Formation, Chesterfield County, South Carolina. Preferred ages (the ages estimated to be the most accurate) are shown in bold (see text for explanation). AGE (ka) MAM = age in thousands of years (ka) ago using the OSL Minimum Age Model-3 for equivalent dose (DE) determinations; AGE (ka) Mean = age in thousands of years (ka) ago using the mean OSL value for equivalent dose (DE) determinations; AGE (ka) Weighted = age in thousands of years (ka) ago using the weighted mean OSL value for equivalent dose (DE) determinations. The ages presented in this table are reported in years before the date of age determination, and are presented with a one-sigma standard deviation of the age uncertainty; DE (Gy) MAM = equivalent dose (grays) using the Minimum Age Model-3 for DE determinations; DE (Gy) Mean = equivalent dose (grays) using the mean OSL value for DE determinations (average of all DE with no filter or model); DE (Gy) Weighted = equivalent dose (grays) using the weighted mean OSL value for DE determinations; disp. (%) = dispersion (percentage) calculated as the average of the equivalent dose divided by the standard deviation of the equivalent dose; (n) DE = number of replicated equivalent dose estimates used to calculate the mean value (total in parentheses denotes the total number of measurements of subsamples or aliquots, including failed runs with unusable data); SITE # (Fig. 3) = OSL site number shown in Fig. 3; USGS ID = U.S. Geological Survey OSL laboratory sample identification code.

USGS ID	SITE # (Fig. 3)	DE (Gy) MAM	DE (Gy) Weighted	DE (Gy) Mean	(n) DE	Disp. (%)	Age (ka) MAM	Age (ka) Weighted	Age (ka) Mean
1585	3	11.20 ± 0.45	12.40 ± 0.58	11.90 ± 0.70	12 (25)	26	**10.16 ± 0.84**	11.27 ± 0.98	10.82 ± 1.02
1586	3	27.50 ± 1.49	12.40 ± 1.15	29.10 ± 1.31	8 (30)	32	**24.09 ± 2.20**	24.12 ± 2.05	25.58 ± 2.22
1588	5	8.08 ± 0.33	8.36 ± 0.39	8.54 ± 0.49	24 (28)	11	9.08 ± 0.80	**9.40 ± 0.82**	9.60 ± 0.89
1589	5	22.60 ± 0.95	23.10 ± 0.87	26.60 ± 1.12	14 (24)	28	**19.32 ± 1.63**	19.65 ± 1.61	22.74 ± 1.91
1642	4	44.40 ± 1.91	44.20 ± 1.14	44.90 ± 3.04	9 (25)	40	**46.29 ± 3.13**	46.04 ± 2.67	46.77 ± 4.00
1643	4	32.90 ± 2.47	32.90 ± 2.47	33.60 ± 1.63	4 (17)	38	**25.50 ± 2.30**	26.46 ± 1.80	25.94 ± 2.30
1715	6	53.70 ± 3.20	63.80 ± 3.19	69.20 ± 3.18	15 (24)	31	**39.80 ± 2.67**	47.30 ± 2.78	51.30 ± 2.85
1716	6	53.20 ± 2.39	59.20 ± 1.36	57.00 ± 1.31	19 (24)	24	62.60 ± 5.64	**69.60 ± 5.65**	67.10 ± 5.46
1717	6	49.90 ± 2.25	44.00 ± 1.23	52.20 ± 1.30	18 (24)	41	**53.70 ± 5.11**	47.30 ± 4.19	56.10 ± 4.90
1718	2	5.78 ± 0.22	6.42 ± 0.38	7.33 ± 0.63	16 (20)	33	**6.96 ± 0.91**	7.73 ± 0.93	8.83 ± 1.33
1719	2	30.20 ± 1.45	30.80 ± 1.45	29.80 ± 1.62	21 (24)	20	47.90 ± 7.59	**48.90 ± 7.73**	47.30 ± 7.59
1720	1	36.50 ± 2.23	49.30 ± 2.22	52.40 ± 2.36	16 (20)	23	36.90 ± 3.16	**49.80 ± 3.74**	53.00 ± 3.89
1721	1	13.80 ± 0.65	15.20 ± 0.58	16.60 ± 0.75	18 (20)	21	8.41 ± 0.60	**9.22 ± 0.61**	10.10 ± 0.71
1722	1	18.80 ± 0.81	18.20 ± 0.82	19.00 ± 0.82	18 (24)	31	**10.90 ± 0.64**	10.60 ± 0.63	11.00 ± 0.64

(SAR) dose protocol (Murray and Wintle, 2000; Wintle and Murray, 2006).

The OSL ages were determined using an exponential and linear fit on the DE data, and the ages are reported in years before the measured date with a one-sigma standard deviation of the age uncertainty (Tables 1 and 2). Determination of DE values was made using the Minimum Age Model-3 (Galbraith and Laslett, 1993; Galbraith et al., 1999), the weighted mean (similar to the Central Age Model of Galbraith et al., 1999), and the mean (average of all DE values with no filter or model). All of the DE determinations and the resultant ages are shown in Table 2.

The dosimetry samples were taken from the tube OSL samples, and thus the dosimetry or dose rate (DR) data were measured from the same sediment as each OSL sample. This sediment was dried, homogenized by disaggregation, weighed, sealed in planchets (techniques modified from Murray et al., 1987), and placed in a gamma-ray spectrometer for determination of elemental concentration of potassium (K), uranium (U), and thorium (Th). Field moisture (water content) was measured from the sediment at the center of each tube in which the sample was collected. Saturation moisture was determined by putting dry sediment in a tube, weighing the tube, filling the tube with water, centrifuging the tube (to simulate compaction), and then draining the water out of the tube and reweighing the sediment. The saturation moisture content is the difference between this new weight and the initial dry sediment weight.

Description of the Carolina Sandhills in the Middendorf and Patrick quadrangles

In the Middendorf and Patrick quadrangles, most of the landscape is covered by a mantle of unconsolidated sand that is mapped as the Pinehurst Formation. At many locations, the unconsolidated sand is <2 m thick and forms a sand sheet of low relief. In areas of

https://doi.org/10.1016/j.yqres.2016.08.007 Published online by Cambridge University Press

higher elevation, however, the unconsolidated sand can be up to 10 m thick and forms subdued hills of up to 6 m relief with steeper sides on the east and southeast (Fig. 6).

The unconsolidated sand (Pinehurst Formation) rests on an unconformity above a unit of sandstone, muddy sandstone to muddy sand, and mud that is mapped collectively as the Cretaceous Middendorf Formation (Fig. 7). There is considerable relief on this unconformity (up to 5 m in places). Most outcrops of the Cretaceous strata consist of grayish red (5R 4/2) to dark yellowish orange (10YR 6/6) medium to coarse sandstone or sand (color nomenclature from Goddard et al., 1963). At many locations, the Cretaceous strata immediately beneath the unconformity display pedogenic mottling, and primary sedimentary structures are not obvious. Sieving analyses of individual samples of Cretaceous sand revealed that the most frequently occurring grain size ranges from medium sand (lower) to coarse sand (lower), and the most frequently occurring sorting values (σ_ϕ) range from 1.01 to 1.80 (poorly sorted). The sand-size grains consist mostly of quartz (99%) with 1% mica and opaque minerals. Most of the quartz grains of medium sand size and coarser are subrounded to subangular, ranging from high sphericity to low sphericity.

The unconsolidated sediment (Pinehurst Formation) above the Cretaceous strata consists of grayish orange (10 YR 7/4) sand. Visual inspection of samples in the field showed that most of the sediment is medium sand (upper) to coarse sand (lower). Sieving analyses revealed that most samples have grain sizes ranging from fine (lower) sand (2.75 ϕ, or 0.149 mm) to coarse (lower) sand (0.75 ϕ, or 0.59 mm), and the most frequently occurring grain size of individual samples ranges from medium (upper) to coarse (lower) sand (1.5–0.74 ϕ, or 0.35–0.59 mm). Sorting values (σ_ϕ) vary from 0.76 to 1.65 (moderately sorted to poorly sorted). The sand-size grains consist predominantly of quartz (99%) with 1% mica and opaque minerals. Most of the quartz grains of medium sand size and coarser are subrounded to subangular, ranging from high sphericity to low sphericity. Textural maturity of the samples ranges from immature to submature.

Exposures of the unconsolidated sand (Pinehurst Formation) do not display primary sedimentary structures, although some structures are visible in GPR data. For example, several GPR traverses across sand hills revealed 2–5-m thick sets of southeast-dipping cross-bedding at depths below 2 m (Fig. 8). Most exposures display evidence of bioturbation by vegetation (plant roots),

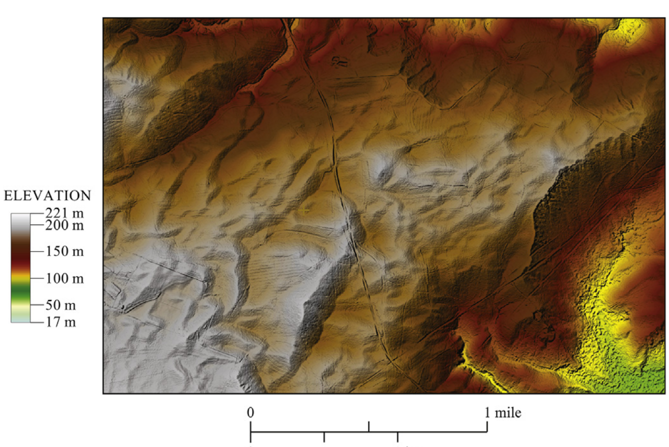

Figure 6. Shaded relief map showing details of "sandhill" morphology in the Middendorf quadrangle, Chesterfield County, South Carolina. Two-meter elevation data are derived from LiDAR point cloud data (South Carolina LiDAR Consortium, 2007, LiDAR and related data products, last accessed July 19, 2015 at http://www.dnr.sc.gov/GIS/lidar.html). Location of image is shown in Fig. 3.

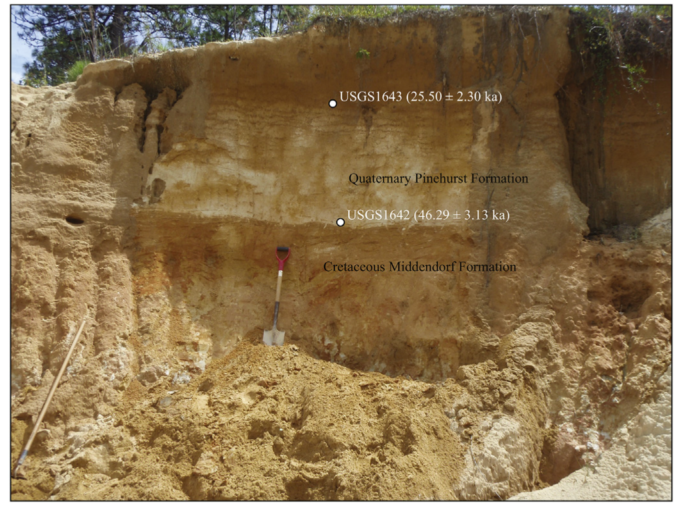

Figure 7. Outcrop of Cretaceous Middendorf Formation, capped by unconformity, which is overlain by Quaternary Pinehurst Formation with OSL ages obtained using the Minimum Age Model-3 (modified from Swezey et al., 2016). Shovel and hoe provide a sense of scale. This location is OSL site #4 (Tables 1 and 2). Location of outcrop is shown in Fig. 3. Similar details about the other OSL sites are available in Swezey et al. (2016).

and pedogenic features such as soil lamellae and modest argillic horizons. Soil types range from deeply weathered plinthitic ultisols to argillic ultisols to sandy entisols, and a few exposures reveal a buried argillic Bt horizon. In the U.S. Department of Agriculture soil survey of Chesterfield County (Morton, 1995), most of the area covered by the Pinehurst Formation is mapped as Alpin sand or Candor sand.

The OSL ages provide an absolute chronology for the Pinehurst Formation. Samples from 6 sites yielded OSL ages ranging from ca. 75 to 6 ka ago (Table 2; Fig. 9). One of these sites is shown in Figure 7, and additional details of these sites are given in Swezey et al. (2016). Using a one-sigma standard deviation of the age uncertainty, one group of OSL ages ranges from ca. 75 to 37 ka, another group of OSL ages ranges from ca. 28 to 18 ka, and a third group of OSL ages ranges from ca. 12 to 6 ka.

Reliability of OSL data

For all OSL samples, the DR results were relatively homogenous (Table 1) and thus several potential problems such as OSL signal variation or disequilibrium in the U–Th decay chain were not considered to be significant impediments to age determination. Some DE recovery tests had less scatter than the natural tests, indicating that some grains in the natural test carried larger luminescence signals. Such larger luminescence signals are thought to have been caused by in-situ dose hot-spots (concentrations of heavy minerals or minerals with large K or U contents) that accumulated during sediment deposition. The larger luminescence signals are not thought to have been caused by partial bleaching (non-zeroing) because: (1) the associated skew and scatter of DE were not indicative of partial bleaching (i.e., there were only a few outliers rather than a uniform skew of progressively larger DE); (2) the DR results were low with observed scattered grains of apatite, potassium feldspar, and zircon; and (3) the dispersion in the results ranged from 11 to 41% (average ~26%). Thus, the most probable cause of the observed patterns of scatter in the DE values is that a few grains of quartz were subjected to increased local radiation by proximity to feldspar or heavy mineral grains.

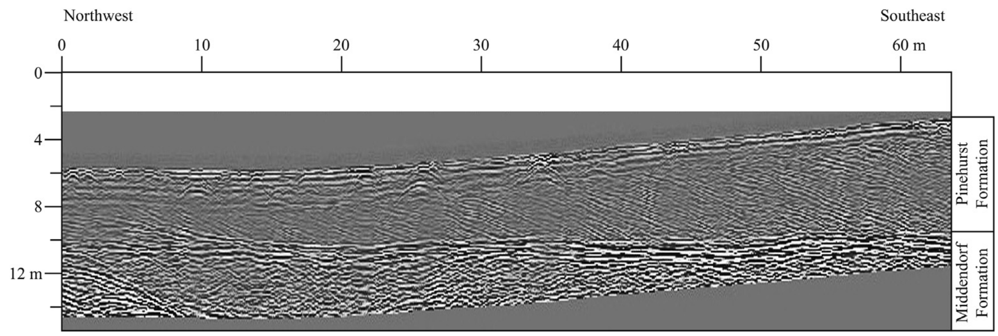

Figure 8. Ground-penetrating radar (GPR) traverse over a sand hill in the Patrick quadrangle, Chesterfield County, South Carolina. Traverse location is shown in Fig. 3.

For many of the samples, the effects of bioturbation on the OSL ages are thought to be negligible because of the absence of the following features that are typically associated with bioturbation (e.g., Bateman et al., 2007a,b): (1) high dispersion values (e.g., consistently >25%); (2) apparently zero-dose grains declining with depth from the surface; (3) significant differences between single grains and single aliquots; and (4) greatly skewed multimodal DE distributions. Some of the OSL samples, however, have relatively high dispersion values (26–41%), which may indicate that some local dose heterogeneity, sediment mixing, or bioturbation has occurred. In these instances, any potential effects of possible bioturbation are not thought to be very great, possibly because bioturbation in the area is caused primarily by plant roots rather than by animal activity that would be more likely to move buried grains to the surface. Three samples from OSL site #6 (USGS1715, -1716, -1717), for example, have significant differences in dispersion values (24%, 31%, and 41%), but relatively similar OSL ages. The similarity of the ages suggests that bioturbation may not be a significant problem, or that bioturbation occurred only within discrete beds. Two samples from OSL site #4 (USGS1642, -1643) also have higher dispersion values (38%, 40%), and it is possible that these samples have been subjected to bioturbation, and thus the ages should be considered to be minimum ages of eolian sediment mobilization. Nevertheless, the ages of these two samples are consistent with the ages of other samples with lower dispersion values. Two samples from OSL site #2 (USGS1718, -1719) have very different dispersion values (20%, 33%), and the sample with the larger dispersion value yielded a very young age of ca. 7 ka. It is possible that this sample has been subjected to bioturbation, and thus the age should be considered to be a minimum age of eolian sediment mobilization. The OSL age of this sample, however, is similar to the age of sample USGS1588 from OSL site #5, which had a dispersion value of only 11%, and thus the age of the sample with the 33% dispersion value (USGS1718) may be reliable.

Table 2 shows separate columns with OSL age estimates according to various statistical models (Minimum Age Model-3, Weighted, Mean). In these columns, the preferred ages (those estimated to be the most accurate) are shown in bold. These preferred ages were chosen as follows: If the dispersion is <25% (as determined by the R program radial plot, following Galbraith and Roberts, 2012), then the preferred age is that obtained by the weighted mean. If the dispersion is $\geq$ 25%, then the preferred age is that obtained by the Minimum Age Model-3. This choice of statistical models for the equivalent dose and the resulting ages follows the recommendations of Galbraith and Roberts (2012) and Reimann et al. (2012), although these authors used a dispersion cutoff value of 20%. For the Carolina Sandhills samples, however, a 20% cutoff value was considered to be too restrictive and a 25% cutoff value was used instead because of the possibility of grains having been mixed in the initial deposit via post-depositional disturbances (as discussed by Galbriath et al., 2012).

Interpretation of depositional environments

The unconsolidated sand (Pinehurst Formation) of the Carolina Sandhills is interpreted as eolian sand sheets and dunes derived from the underlying Cretaceous sand, mobilized repeatedly during conditions of colder temperatures and reduced vegetation cover, and then subsequently degraded and stabilized by pedogenesis and vegetation. As outlined below, the eolian interpretation of the Pinehurst Formation is derived from an assemblage of the following five characteristics: (1) sandhill location; (2) sandhill morphology and primary sedimentary structures; (3) OSL ages; (4) grain-size data; and (5) bioturbation and pedogenic features. Any one of these characteristics alone is not necessarily diagnostic of an eolian depositional environment, but the total assemblage of these characteristics, as well as the overall setting and relations with underlying strata, suggest that an eolian interpretation is most likely.

Sandhill location

The location of the Pinehurst Formation places some constraints on possible sediment sources and rules out some depositional environments. For example, the sand of the Pinehurst Formation is not located adjacent to obvious Quaternary fluvial channels that might have provided a sediment source. However, the sand is located exclusively in areas where the Cretaceous Middendorf Formation is near the surface (noted by Cooke, 1936; Ridgeway et al., 1966). This spatial association of the Pinehurst Formation with outcrops of the Cretaceous sandstone and sand strongly suggests that the Pinehurst Formation was derived from the underlying Cretaceous strata.

Sandhill morphology and primary sedimentary structures

In relatively flat topographically high areas, the sand of the Pinehurst Formation forms hills of up to 6 m relief, with steeper sides on the east and southeast (Fig. 6). Although primary sedimentary structures are not visible in exposures of the Pinehurst Formation, the steeper sides of the hills being on the east and southeast is consistent with dip directions of cross-bedding in GPR data (Fig. 8), thus suggesting that the hill morphology is relict depositional topography of bedforms (dunes) rather than erosional topography unrelated to depositional processes. Furthermore, if the steeper sides of the hills are the lee sides of bedforms, then the fluid that mobilized the bedforms would have flowed from west to east and (or) northwest to southeast.

https://doi.org/10.1016/j.yqres.2016.08.007 Published online by Cambridge University Press

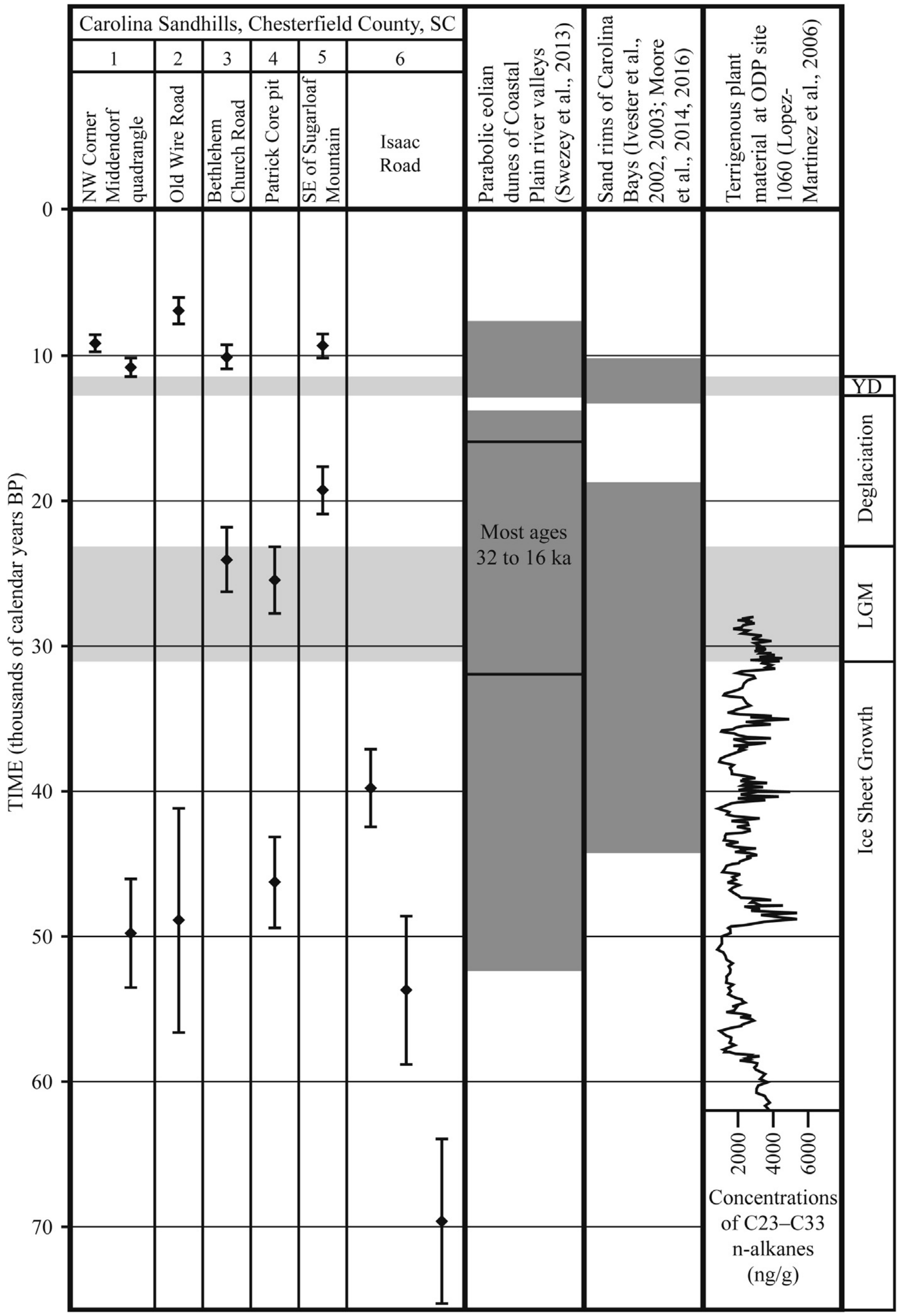

Figure 9. Chart of OSL ages from the Carolina Sandhills (using the preferred OSL ages as indicated in Table 2), OSL ages from parabolic eolian dunes in coastal plain river valleys (from Swezey et al., 2013), and OSL ages from eolian sand rims of Carolina Bays (from Ivester et al., 2002, 2003; Moore et al., 2014, 2016), as well as evidence for wind activity from ODP site 1060 (from Lopez-Martinez et al., 2006). The numbers above the Carolina Sandhills columns refer to OSL sites shown in Fig. 3. Data for these samples are given in Tables 1 and 2. LGM = last glacial maximum; YD = Younger Dryas event.

OSL ages

The OSL ages from the Pinehurst Formation range from ca. 75 to 6 ka ago (Table 2; Fig. 9), and thus provide some constraints on possible depositional environments. Most of the OSL ages range from ca. 75 to 22 ka, and are approximately coincident with ice sheet growth and the last glacial maximum (LGM) in the northern hemisphere, using the dates of ca. 115 ka for the inception of the Laurentide Ice Sheet (Mix, 1992; Kleman et al., 2010) and ca. 31,100 to 23,200 calibrated years before present (cal yr BP) for the LGM [reported by Clark et al. (2009) as 26.5 to 19–20 ka in radiocarbon years before present (^{14}C yr BP), and converted to cal yr BP using the program CALIB 6.1.1 (available at http://calib.qub.ac.uk/calib), in conjunction with Stuiver and Reimer (1993) and Reimer et al. (2009)]. There are apparent gaps in the OSL ages from ca. 37 to 28 ka and from ca. 18 to 12 ka. A final episode of eolian sediment mobilization is revealed by several OSL ages ca. 12 to 6 ka. Most of these ages are approximately coincident with the interval from the Younger Dryas event, which is dated at 12,800 to 11,500 cal yr BP (Alley et al., 1993), through the final collapse of the Laurentide Ice

https://doi.org/10.1016/j.yqres.2016.08.007 Published online by Cambridge University Press

Sheet, which is dated at ca. 8.2 ka (Barber et al., 1999; Shuman et al., 2002). No OSL ages from the study area are younger than ca. 6 ka, and thus it appears that since this date the dune morphology has been degraded, and the sand has been stabilized by vegetation and subjected to pedogenic processes.

The OSL ages rule out the possibility of the Pinehurst Formation being beach deposits because sea level was well below the elevation of the Carolina Sandhills region during the time of the OSL ages. Likewise, the OSL ages rule out the possibility of the sand being associated with the Chesapeake Bay impact crater, which formed during the Eocene (Powars, 2000). The OSL ages also rule against fluvial deposits because the sand blankets most of the landscape and is not spatially associated with obvious fluvial channels. Furthermore, the OSL ages from the Pinehurst Formation are coincident with OSL ages from other known eolian features elsewhere in the southeastern United States (e.g., Ivester et al., 2001; Swezey et al., 2013; Markewich et al., 2015; Moore et al., 2016).

Grain-size data

In the Middendorf and Patrick quadrangles, the Pinehurst Formation consists primarily of moderately sorted to poorly sorted medium sand (upper) to coarse sand (lower). The relatively coarse grain size and poor sorting suggest that the sand has not traveled very far from its source, which is believed to be the underlying Cretaceous sand. The interpretation that the Pinehurst Formation is derived from the underlying Cretaceous sand is strengthened by the fact that sand of the Pinehurst Formation has only slightly finer grain size modes and only slightly better sorting than the Cretaceous sand. This conclusion is consistent with observations by Ridgeway et al. (1966), who noted that the two units (Pinehurst Formation and underlying Middendorf Formation) have similar grain sizes and similar abundance and composition of heavy minerals.

For the interpretation of an eolian environment, the Pinehurst Formation grain-size data can appear to be misleading at first because many eolian sediments are moderately sorted to well sorted fine sand (e.g., Ahlbrandt, 1979; Goudie and Watson, 1981; Lancaster, 1986, 1989; Goudie et al., 1987). A search of the literature, however, reveals numerous examples of relatively coarse-grained eolian sand dunes and sand sheets. Restricting the discussion to quartz grains, eolian dunes composed of predominantly coarse sand have been described from several cold-climate settings such as Colorado in the United States (Ahlbrandt, 1979; Fryberger et al., 1979), the east side of Hudson Bay in Canada (Ruz and Allard, 1995), and the coasts of England and Denmark (Knight et al., 1998; Saye and Pye, 2006; Clemmensen et al., 2007). Eolian sand sheets and (or) wind ripples composed of coarse sand to granule size grains have been described from several cold-climate settings such as Colorado (Andrews, 1981), various locations in Canada (Cailleux, 1974; Good and Bryant, 1985; McKenna-Neuman and Gilbert, 1986; McKenna Neuman, 1990; Germain and Filion, 2002), Greenland (Willemse et al., 2003), Scotland (Ballantyne and Whittington, 1987), and Antarctica (Calkin and Rutford, 1974; Selby et al., 1974; Ackert, 1989; Gillies et al., 2012).

Many examples of relatively coarse eolian sediments are from cold environments because cold winds are more effective at eolian transport than warm winds (Selby et al., 1974; McKenna Neuman, 1989, 1993, 2003, 2004). Specifically, grain impacts on cold surfaces are more elastic than impacts on warm surfaces. Furthermore, as air temperature decreases, there is an increase in air density, an increase in turbulence intensity of the air flow, a decrease in air viscosity, a decrease in the amount of water vapor in the air, and a decrease in cohesion among grains. Air density is proportional to the drag force on a grain moving in air, and thus as air density increases there is a decrease in the threshold shear velocity and an increase in the movement of relatively coarse grains for any given drag velocity. In other words, it is easier to entrain particles at lower temperatures. As a specific example, wind tunnel experiments have shown that -12°C air can entrain particles 40–50% larger in diameter than $+32^{\circ}$C air (McKenna Neuman, 2003).

As a final comment about grain-size data, a previous study of the Carolina Sandhills used moment method statistics to create bivariate plots of grain-size data (mean grain size, sorting, kurtosis, skewness), and these plots were then used to make interpretations of depositional environments (Leigh, 1998). The interpretation of such plots is based on claims that they yield viable information for discriminating depositional environments (e.g., Friedman, 1961, 1979; Moiola and Weiser, 1968; Moiola et al., 1968). However, many subsequent studies using different bivariate plots have revealed no distinct segregation of data according to depositional environment (Slee et al., 1964; Gees, 1965; Solohub and Klovan, 1970; Glaister and Nelson, 1974; Stapor and Tanner, 1975; Taira and Scholle, 1979; Tucker and Vacher, 1980; Thomas, 1987). Despite a long history of attempts to use bivariate plots of grain-size data to identify depositional environments, the general conclusion from these studies is that bivariate plot field boundaries for depositional environments are subjective and not reliable, and their use results in oversimplification and ambiguous (or contradictory) results (Amaral and Pryor, 1977; Tucker and Vacher, 1980; Ehrlich, 1983; Forrest and Clark, 1989).

Bioturbation and pedogenic features

The lack of primary sedimentary structures in exposures of the Pinehurst Formation is attributed to bioturbation (plant roots) and pedogenesis, which can be common in vegetated eolian sands (e.g., Glennie and Evamy, 1968; Ahlbrandt et al., 1978). Certain pedogenic features such as soil lamellae and modest argillic Bt horizons may indicate a lower limit to significant bioturbation, especially at locations where these features appear 1–2 m below the ground surface. Buried Bt horizons are visible in several exposures of the Candor soil series (Morton, 1995; Whittecar and Fitzwater, 2016). These pedogenic features and the lack of obvious primary sedimentary structures in the upper few meters of the Pinehurst Formation suggest that the surfaces of sand sheets and dunes were stabilized by vegetation during one or more episodes for a duration long enough to form soil profiles and for bioturbation to obliterate primary sedimentary structures.

Discussion

The OSL ages suggest that there may have been several episodes of eolian sediment mobilization in the Carolina Sandhills region. One group of ages ranges from ca. 75 to 37 ka (coincident with ice sheet growth in the northern hemisphere), and another group of ages ranges from ca. 28 to 18 ka (approximately coincident with the LGM in the northern hemisphere). There appear to be gaps in the OSL ages from ca. 37 to 28 ka and from ca. 18 to 12 ka. It is possible that the eolian sediment may have been stabilized during these times, but it is also possible that additional OSL ages may fill in these gaps.

The interpretation of the Carolina Sandhills (Pinehurst Formation) as eolian sand sheets and dunes is consistent with other evidence for eolian activity in the southeastern United States during the last glaciation. For example, parabolic eolian dunes were active ca. 40 to 19 ka in river valleys of the coastal plain from Georgia to Delaware (Markewich and Markewich, 1994; Ivester et al., 2001; Swezey et al., 2013; Markewich et al., 2015). Additional evidence comes from Carolina Bays, where eolian sand ridges on the southeast margins of various bays have yielded OSL ages ranging from ca. 44.3 to 18.8 ka (Ivester et al., 2002, 2003; Moore et al., 2014, 2016). In addition, compounds of higher terrestrial plants off the east coast of the United States at Blake Outer Ridge (ODP Site 1060, ~31° N latitude) provide a record of several abrupt changes in westerly winds from ca. 60 to 30 ka (Lopez-Martinez et al., 2006). At this site, greater concentrations of terrestrial plant compounds (derived from the continent by eolian processes) are correlated with cold events and stronger westerly winds blowing off the continent.

A subsequent episode of eolian mobilization of the Pinehurst Formation is revealed by several OSL ages ranging from ca. 12 to 6 ka, and most of these ages are approximately coincident with the Younger Dryas (ca. 12,800 to 11,500 cal yr BP) through the final collapse of the Laurentide Ice Sheet at ca. 8.2 ka. Of the six sites with multiple OSL ages in vertical succession (Fig. 9), the uppermost age at four sites falls within this ca. 12 to 6 ka range. It is possible that eolian sand mobilization began at many places in the study area during the Younger Dryas, and that the OSL ages indicate not the total time of eolian sand mobilization but only the time that eolian mobilization ceased at specific sites. The interpretation of eolian sediment mobilization during the Younger Dryas in the Carolina Sandhills is consistent with evidence for eolian mobilization of dunes on the floodplain of the Savannah River ca. 14.4 to 11.4 ka (Swezey et al., 2013) and eolian mobilization of Carolina Bay sand rims ca. 13.6 to 10.3 ka (Ivester et al., 2002, 2003; Moore et al., 2014, 2016).

Finally, no OSL ages from the Pinehurst Formation are younger than ca. 6 ka, and thus it appears that since this date the sand has remained stabilized by vegetation and has been subjected to pedogenic processes. In other words, climate changes since ca. 6 ka have not exceeded thresholds for eolian mobilization of the sand.

Vegetation during episodes of eolian sediment mobilization

Some eolian sand sheets may develop simply because of coarse grain size, whereas others may develop because of a combination of coarse grain size and the presence of vegetation (Kocurek and Nielson, 1986). In the case of the Carolina Sandhills, it seems likely that some vegetation was present when the eolian sand was mobile. The paleosols in the study area imply the presence of forests that were capable of producing enough organic litter during a long enough time to generate the acids needed to form Bt soil horizons.

Coincident with the proposed eolian activity during the last glaciation, pollen data from nearby sites within the Carolina Sandhills indicate that from ca. 22,860 to 20,750 cal yr BP the region was dominated by a forest of boreal spruce and pine (Watts, 1980; Taylor et al., 2011), although the tree cover then was much less dense than in modern boreal forests (Watts, 1983; Overpeck et al., 1992; Cowling, 1999; Williams et al., 2000; Williams, 2002). Data reported by Watts (1980) from White Pond (Kershaw County, SC) approximately 70 km SW of the Middendorf quadrangle indicate that the time interval of ca. 19,100 ^{14}C yr BP (ca. 22,860 cal yr BP) was characterized by high abundance of spruce (*Picea*) and pine (*Pinus*), low abundance of oak (*Quercus*), and absence of hickory (*Carya*) and beech (*Fagus*). Likewise, data reported by Taylor et al. (2011) from Ft. Jackson (Richland County, SC) approximately 90 km SW of the Middendorf quadrangle indicate that the time interval of ca. 18,100 to 17,400 ^{14}C yr BP (ca. 21,650 to 20,750 cal yr BP) was characterized by high abundance of spruce and pine, low abundance of oak, and absence of beech. They interpreted this taxa association (especially the abundant spruce with pine) as being correlative with a dry and cool climate. In contrast, however, the interpretation of dry conditions during the last glaciation is not consistent with interpretations by Leigh and Feeney (1995) of greater precipitation ca. 31 to 28 ka on the basis of fluvial paleochannel morphologies in Georgia.

Although not a record of great resolution, data from White Pond indicate that the time interval of ca. 12,800 to 9550 ^{14}C yr BP (ca. 15,400–14,300 to 11,000–10,800 cal yr BP) was characterized high abundance of hickory, beech, and oak, low abundance of pine, and absence of spruce (Watts, 1980). This interval encompasses both the time of deglaciation and the Younger Dryas (Fig. 9).

Coincident with a proposed subsequent episode of eolian activity during the Younger Dryas through the final collapse of the Laurentide Ice Sheet, high-resolution pollen records from Florida indicate that the Younger Dryas was dry and cool, with an initial slightly drier phase ca. 12.9 to 12.3 ka and a later significantly drier phase ca. 12.3 to 11.4 ka (Willard et al., 2007; Bernhardt et al., 2012). In contrast, some lower-resolution pollen studies from fluvial settings have suggested that the Younger Dryas may have been moist and cool in the southeastern United States (e.g., LaMoreaux et al., 2009). Yet other studies have concluded that the Younger Dryas record is not readily apparent in the regional fluvial record (e.g., Leigh, 2008).

Post-Younger Dryas pollen data from the Carolina Sandhills are reported from Ft. Bragg (Cumberland County, NC) approximately 125 km NE of the Middendorf quadrangle, and from Ft. Jackson (Richland County, SC). The data from Ft. Bragg indicate that the time interval of ca. 9110 ^{14}C yr BP (ca. 10,270 to 10,210 cal yr BP) was characterized by relatively high abundance of pine and low abundance of oak, whereas the time interval of ca. 8950 to 8420 ^{14}C yr BP (ca. 10,210 to 9310 cal yr BP) was characterized by relatively low abundance of pine and increased abundance of oak (Goman and Leigh, 2004). Likewise, the data from Ft. Jackson indicate that the time interval of ca. 8900 to 5800 ^{14}C yr BP (ca. 10,020 to 6660 cal yr BP) was characterized by high abundance of oak and beech, low abundance of pine, and absence of spruce (Taylor et al., 2011). The authors interpreted the greater abundance of oak as being correlative with greater precipitation and a warmer climate. This interpretation of greater precipitation during the early Holocene is consistent with conclusions by Leigh and Feeney (1995) on the basis of fluvial paleochannel morphologies in Georgia.

A compilation of regional pollen data suggests that during the LGM the tree species of Chesterfield County were dominated by jack pine (*Pinus banksiana*), that spruce composed approximately 10% of the trees, and that fir (*Abies*) composed approximately 3–4% of the trees (Delcourt and Delcourt, 1985). For comparison, jack pine is the dominant tree today in boreal forests of southern Manitoba and east-central Ontario (Whitehead, 1973; Delcourt and Delcourt, 1985). Sand plains similar to the Carolina Sandhills are a favored habitat of jack pine in the Great Lakes region of North America (Watts, 1980).

According to pollen data, the southern limit of the boreal forest during the LGM was located at ~33–34° N latitude (Delcourt and Delcourt, 1983, 1984, 1985). Woodcock and Wells (1990) place this boundary closer to 33° N latitude (Fig. 10). For comparison, this boundary in North America today is located in northern Michigan and southern Ontario at ~47–48° N latitude (Brandt, 2009). Although Brandt (2009) cautions that extremes of weather rather than mean conditions may be more important for governing the distribution of plants, the southern boundary of the boreal forest today corresponds with an average number of 120 frost-free days (Watts, 1983) and a mean temperature of 20°C for the warmest month (Wolfe, 1979). An LGM July temperature of 20°C at 33° N latitude is only slightly different from estimates by Jackson et al. (2000), who indicated that the area of Chesterfield County had a mean LGM July temperature of ca. 21°C and a mean LGM January temperature of ca. −17°C (Fig. 10).

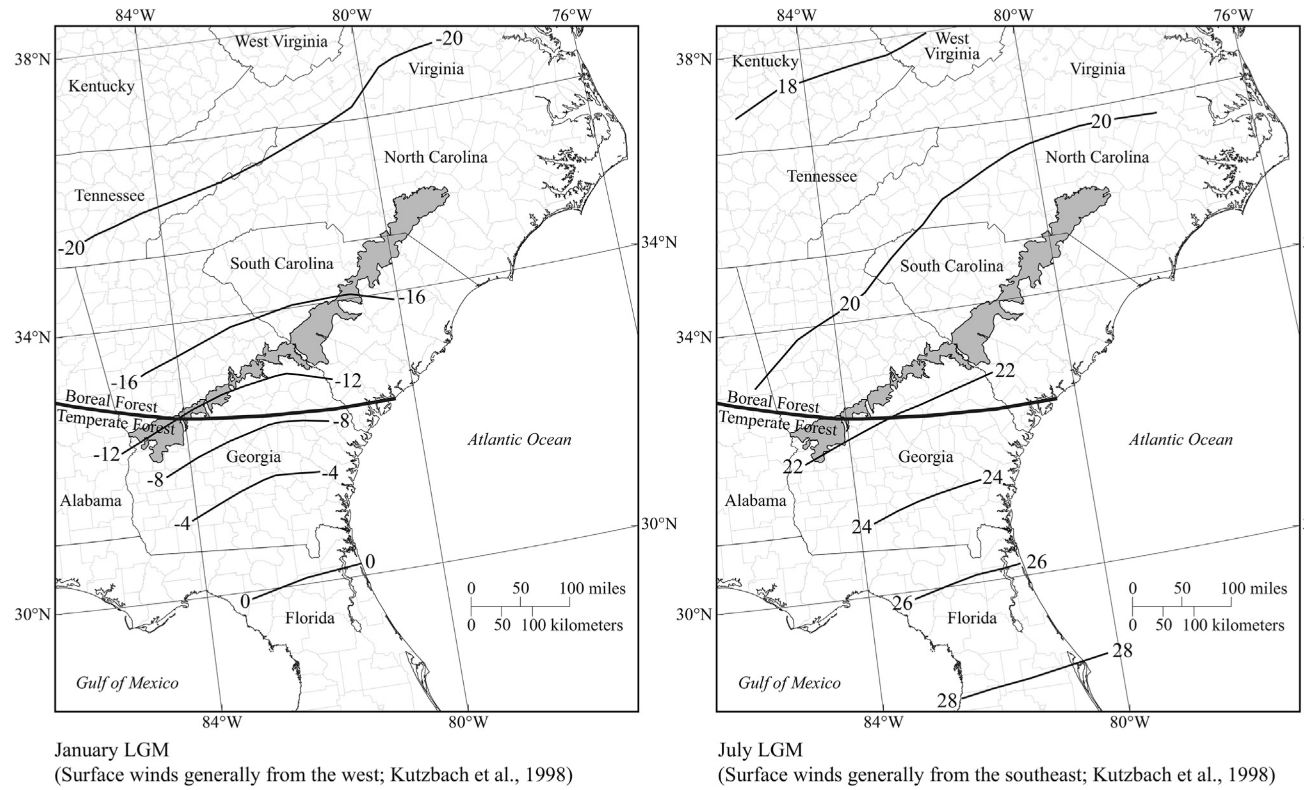

Figure 10. Estimates of paleoclimate conditions for January and July during the last glacial maximum. Shaded area denotes the Carolina Sandhills. Temperature estimates in degrees Celsius are from Jackson et al. (2000). Southern limit of boreal forest is from Woodcock and Wells (1990).

Paleo-wind interpretations

In addition to temperature parameters, the southern boundary of the boreal forest today corresponds with the mean winter position of the polar front jet stream (Delcourt and Delcourt, 1983, 1984, 1985). If this coincidence also occurred during the LGM, then the mean winter position of the polar front jet stream during the LGM would have been located at ~33–34° N latitude. This interpretation is consistent with many climate models, which suggest that the polar front jet stream and the westerlies shifted to lower latitudes during the LGM (CLIMAP, 1976; Gates, 1976; McIntyre et al., 1976; Street and Grove, 1979; Broccoli and Manabe, 1987; COHMAP Members, 1988; Kutzbach et al., 1993, 1998; Bartlein et al., 1998; Whitlock et al., 2001; Shin et al., 2003; Otto-Bliesner et al., 2006; Li and Battisti, 2008).

In Chesterfield County, the relict dune morphologies are consistent with winds that mobilized these dunes blowing from west to east and (or) from northwest to southeast. These interpretations of wind direction are consistent with previous studies of parabolic eolian dunes in coastal plain river valleys that suggest that the winds that mobilized the river valley dunes blew from the west in Georgia, that the winds shifted gradually across the Carolinas to blow from the southwest in North Carolina, and that the winds blew from the northwest in Maryland and Delaware (Carver and Brook, 1989; Markewich and Markewich, 1994; Ivester and Leigh, 2003; Swezey et al., 2013).

The dune morphologies of the Carolina Sandhills (Pinehurst Formation) are more consistent with modern January wind directions than July wind directions (Fig. 4), prompting speculation that dune mobilization may have occurred preferentially during the winter. Consistent with modern wind directions, models by Kutzbach et al. (1998) suggest that surface winds in the southeastern United States blew generally from the west during the LGM winter and from the southeast during the LGM summer (Fig. 10). Under modern conditions, the westerlies and the polar front jet stream are certainly stronger during winter than summer. Furthermore, the Bermuda High (which dominates much of the present summer wind behavior) is thought to have been weaker during the LGM (Oglesby et al., 1989; Bartlein et al., 1998) and/or is thought to have been displaced to the east relative to its position today (Forman et al., 1995).

The relatively coarse grain size of the Pinehurst Formation (mean range of 0.35–0.59 mm) provides some indication of wind velocities that might have mobilized the sand. In relatively warm low-latitude regions, typical threshold wind velocities for sustained eolian mobilization of 0.25–0.50 mm diameter quartz sand are 4–6 m/sec (e.g., Hsu, 1974). Fryberger and Dean (1979), for example, used a threshold wind velocity of 11.6 knots (6 m/sec) in their calculations of a threshold wind velocity for eolian sediment drift potential of 0.25–0.33 mm diameter quartz sand. In the Carolina Sandhills, modern wind velocities of 6 m/sec or greater occur approximately 8% of the time per whole year (Weber et al., 2003) (www.ncdc.noaa.gov; accessed 18 August 2016). This low frequency of modern higher-velocity winds does not necessarily preclude modern eolian sand transport in the Carolina Sandhills. For example, in a study from the Ordos Plateau in China, Liu et al. (2005) documented eolian mobilization of dune sand, even though the total duration of sand-transporting winds was 8.4% of the year at one location where the vegetation cover ranged mostly from semi-fixed (5–50%) to fixed (>50%) and 6.6% of the year at another location where the vegetation cover ranged mostly from shifting (<5%) to semi-fixed (5–50%). Nevertheless, none of the OSL ages from the Carolina Sandhills is younger than ca. 6 ka.

With regards to eolian mobilization of 0.35–0.59 mm diameter sand during the LGM, it is important to consider the effects of air temperature, which would have been much cooler than modern

https://doi.org/10.1016/j.yqres.2016.08.007 Published online by Cambridge University Press

temperatures. As mentioned above, it is easier to entrain particles at lower air temperatures, and experiments have shown that −12°C air can entrain particles 40–50% larger in diameter than +32°C air (McKenna Neuman, 2003). Thus, as a rough approximation, the wind velocity required for sustained eolian mobilization of 0.35–0.59 mm diameter sand (mean size range of the Pinehurst Formation) during the LGM winter (January temperature of ca. −17°C, according to Jackson et al., 2000) would have been approximately the same as the wind velocity required for sustained eolian mobilization of 0.25–0.50 mm diameter sand under relatively warm conditions today (such as those investigated by Hsu, 1974). In other words, sustained eolian mobilization of the Carolina Sandhills (Pinehurst Formation) during the LGM winter would have required wind velocities of at least 4–6 m/sec. Air temperatures during the LGM summer would have been warmer, and thus even greater wind velocities would have been required to mobilize the sand during the LGM summer.

Conclusions

The Carolina Sandhills is a 15–60 km wide physiographic region of abundant sand that extends from the western border of Georgia to central North Carolina in the updip portion of the Atlantic Coastal Plain province of the southeastern United States. In Chesterfield County of South Carolina, the “sandhills” consist of moderately sorted to poorly sorted medium to coarse sand. This unconsolidated sand is mapped as the Pinehurst Formation, and is interpreted as eolian sand sheets and dunes derived from the underlying Cretaceous sand during conditions of cooler temperatures and reduced vegetation cover. OSL ages indicate that there have been several episodes of eolian sand mobilization. Two sets of OSL ages range from ca. 75 to 37 ka and 28 to 18 ka, and are generally coincident with growth of the Laurentide Ice Sheet and the last glacial maximum (LGM). Another set of OSL ages ranges from ca. 12 to 6 ka and most of these ages are coincident with the Younger Dryas event through final collapse of the Laurentide Ice Sheet. These OSL ages from the Carolina Sandhills are coincident with other evidence for eolian sediment mobilization in the southeastern United States during this time (e.g., parabolic eolian dunes in coastal plain river valleys, Carolina Bays). Since ca. 6 ka, however, eolian dune morphologies have been degraded, and the sand has been stabilized by vegetation and subjected to pedogenic processes. This stabilization by vegetation has occurred in association with a general increase in air temperature, an increase in vegetation density, and an overall change to a less arid climate.

Although dunes are less common than sand sheets within the Carolina Sandhills, the relict dune morphologies and cross-bedding are consistent with winds blowing from the west and (or) northwest. These inferred wind directions are most consistent with modern January wind directions and inferred LGM January wind directions, suggesting that eolian sand mobilization may have occurred preferentially during the winter. The predominance of sand sheets over dunes is attributed to the coarse grain size and to the likely presence of some vegetation when the sand was mobilized (although vegetation density would have been less than it is today). Finally, the relatively coarse grain size suggests that eolian sand mobilization during the LGM winter would have required wind velocities of at least 4–6 m/sec, after taking into account the effects of colder air temperatures on eolian sand transport.

Acknowledgments

The authors thank Allyne Askins, Nancy Jordan, and Jack Culpeper (Carolina Sandhills National Wildlife Refuge) and Brian Davis (Carolina Sand Hills State Forest), as well as numerous landowners in Chesterfield County, for property access and permission to work at various locations. BAF and GRW received USGS EdMap funding for geologic mapping of the Patrick quadrangle (Chesterfield County, SC). This manuscript benefitted from reviews by USGS geologists Christopher Bernhardt and Thomas Cronin, as well as reviews for the journal by Joe Mason, an anonymous reviewer, and journal editors James Shulmeister and Derek Booth. Any use of trade, firm, or product names is for descriptive purposes only and does not imply endorsement by the U.S. Government.

References

Ackert Jr., R.P., 1989. The origin of isolated gravel ripples in the western Asgard Range, Antarctica. Antarctic Journal of the United States 24 (5), 60–62.
Ahlbrandt, T., 1979. Textural parameters of eolian deposits. In: McKee, E. (Ed.), A Study of Global Sand Seas, U.S. Geological Survey Professional Paper 1052, pp. 21–51.
Ahlbrandt, T.S., Andrews, S., Gwynne, D.T., 1978. Bioturbation in eolian deposits. Journal of Sedimentary Petrology 48, 839–848.
Alley, R., Meese, D., Shuman, C., Gow, A., Taylor, K., Grootes, P., White, J., Ram, M., Waddington, E., Mayewski, P., Zielinski, G., 1993. Abrupt increase in Greenland snow accumulation at the end of the Younger Dryas event. Nature 362, 527–529.
Amaral, E.J., Pryor, W.A., 1977. Depositional environment of the St. Peter Sandstone deduced by textural analysis. Journal of Sedimentary Petrology 47, 32–52.
Andrews, S., 1981. Sedimentology of Great Sand Dunes, Colorado. In: Ethbridge, F.G., Flores, R.M. (Eds.), Recent and Ancient Nonmarine Depositional Environments: Models for Exploration. SEPM Special Publication 31, pp. 279–291.
Baldwin, J.L., 1975. Weather Atlas of the United States. Gale Research Company, Detroit, MI (262 pp.).
Ballantyne, C.K., Whittington, G., 1987. Niveo-aeolian sand deposits on An Teallach, Wester Ross, Scotland. Transactions of the Royal Society of Edinburgh: Earth Sciences 78, 51–63.
Barber, D.C., Dyke, A., Hillaire-Marcel, C., Jennings, A.E., Andrews, J.T., Kerwin, M.W., Bilodeau, G., McNeely, R., Southon, J., Morehead, M.D., Gagnon, J.-M., 1999. Forcing of the cold event of 8,200 years ago by catastrophic drainage of Laurentide lakes. Nature 400, 344–348.
Bartlein, P.J., Anderson, K.H., Anderson, P.M., Edwards, M.E., Mock, C.J., Thompson, R.S., Webb, R.S., Webb III, T., Whitlock, C., 1998. Paleoclimate simulations for North America over the past 21,000 years: features of the simulated climate and comparisons with paleoenvironmental data. Quaternary Science Reviews 17, 549–585.
Bartlett Jr., C.S., 1967. Geology of the Southern Pines Quadrangle (M.S. thesis). The University of North Carolina at Chapel Hill, North Carolina (101 pp.).
Bateman, M.D., Boulter, C.H., Carr, A.S., Frederick, C.D., Peter, D., Wilder, M., 2007a. Detecting post-depositional sediment disturbance in sandy deposits using optical luminescence. Quaternary Geochronology 2, 57–64.
Bateman, M.D., Boulter, C.H., Carr, A.S., Frederick, C.D., Peter, D., Wilder, M., 2007b. Preserving the palaeoenvironmental record in drylands: bioturbation and its significance for luminescence-derived chronologies. Sedimentary Geology 195, 5–19.
Bernhardt, C.E., Willard, D.A., Gifford, J., 2012. Pollen evidence for a cool, dry Younger Dryas and warm, wet early Holocene in the southeastern United States. Palynological Society of Japan, IPC-XIII/IOPC-IX Abstracts 58, 15–16.
Brandt, J.P., 2009. The extent of the north American boreal forest. Environmental Reviews 17, 101–161.
Broccoli, A.J., Manabe, S., 1987. The influence of continental ice, atmospheric CO_2, and land albedo on the climate of the last glacial maximum. Climate Dynamics 1, 87–99.
Cailleux, A., 1974. Formes précoces et albedos du nivéo-éolien. Zeitschrift für Geomorphologie 18, 437–459.
Calkin, P.E., Rutford, R.H., 1974. The sand dunes of Victoria Valley, Antarctica. Geographical Review 64, 189–216.
Carver, R.E., Brook, G.A., 1989. Late Pleistocene paleowind directions, Atlantic Coastal Plain, U.S.A. Palaeogeography, Palaeoclimatology, Palaeoecology 74, 205–216.
Christensen, N.L., 2000. Vegetation of the southeastern Coastal Plain. In: Barbour, M.G., Billings, W.D. (Eds.), North American Terrestrial Vegetation, second ed. Cambridge University Press, Cambridge, pp. 397–448.
Clark, P.U., Dyke, A.S., Shakun, J.D., Carlson, A.E., Clark, J., Wohlfarth, B., Mitrovica, J.X., Hostetler, S.W., McCabe, A.M., 2009. The last glacial maximum. Science 325, 710–714.
Clemmensen, L.B., Bjørnsen, M., Murray, A., Pedersen, K., 2007. Formation of aeolian dunes on Anholt, Denmark since AD 1560: a record of deforestation and increased storminess. Sedimentary Geology 199, 171–187.
CLIMAP Project Members, 1976. The surface of the ice-age earth. Science 191, 1131–1137.

COHMAP Members, 1988. Climate changes of the last 18,000 years: observations and model simulations. Science 241, 1043–1052.
Conley, J.F., 1962. Geology and mineral resources of Moore County, North Carolina. North Carolina Division of Mineral Resources Bulletin 76 (40 pp.).
Cooke, C.W., 1936. Geology of the Coastal Plain of South Carolina. U.S. Geological Survey Bulletin 867 (196 pp.).
Court, A., 1974. The climate of the conterminous United States. In: Bryson, R.A., Kare, F.K. (Eds.), Climates of North America. Elsevier, Amsterdam, pp. 193–343.
Cowling, S.A., 1999. Simulated effects of low atmospheric CO_2 on structure and composition of north American vegetation at the last glacial maximum. Global Ecology and Biogeography 8, 81–93.
Davis, R.E., Hayden, B.P., Gay, D.A., Phillips, W.L., Jones, G.V., 1997. The north Atlantic subtropical anticyclone. Journal of Climate 10, 728–744.
Delcourt, P.A., Delcourt, H.R., 1983. Late-Quaternary vegetational dynamics and community stability reconsidered. Quaternary Research 19, 256–271.
Delcourt, H.R., Delcourt, P.A., 1985. Quaternary palynology and vegetational history of the southeastern United States. In: Bryant Jr., V.M., Holloway, R.G. (Eds.), Pollen Records of Late-Quaternary North American Sediments. American Association of Stratigraphic Palynologists Foundation, Dallas, TX, pp. 1–37.
Delcourt, P.A., Delcourt, H.R., 1984. Late Quaternary paleoclimates and biotic responses in eastern north America and the western north Atlantic Ocean. Palaeogeography, Palaeoclimatology, Palaeoecology 48, 263–284.
Dowsett, H.J., Cronin, T.M., 1990. High eustatic sea level during the middle Pliocene: evidence from the southeastern U.S. Atlantic Coastal Plain. Geology 18, 435–438.
Earley, L.S., 2004. Looking for Longleaf: the Fall and Rise of an American Forest. The University of North Carolina Press, Chapel Hill, North Carolina (336 pp.).
Ehrlich, R., 1983. Size analysis wears no clothes, or have moments come and gone? Journal of Sedimentary Petrology 53, 1.
Fitzwater, B.A., 2016. Reevaluating the Geologic Formations of the Upper Coastal Plain in Chesterfield County, South Carolina (M.S. thesis). Old Dominion University, Norfolk, Virginia (130 pp.).
Folk, R.L., 1951. Stages of textural maturity in sedimentary rocks. Journal of Sedimentary Petrology 21, 127–130.
Folk, R.L., 1954. The distinction between grain size and mineral composition in sedimentary rock nomenclature. Journal of Geology 62, 344–359.
Folk, R.L., 1956. The role of texture and composition in sandstone classification. Journal of Sedimentary Petrology 26, 166–171.
Folk, R.L., 1966. A review of grain size parameters. Sedimentology 6, 73–93.
Folk, R.L., 1980. Petrology of Sedimentary Rocks. Hemphill Publishing Company, Austin, TX (170 pp.).
Folk, R.L., Ward, W.C., 1957. Brazos River point bar: a study in the significance of grain size parameters. Journal of Sedimentary Petrology 27, 3–26.
Folk, R.L., Andrews, P.B., Lewis, D.W., 1970. Detrital sedimentary rock classification and nomenclature for use in New Zealand. New Zealand Journal of Geology and Geophysics 13, 937–968.
Forman, S.L., Oglesby, R., Markgraf, V., Stafford, T., 1995. Paleoclimatic significance of Late Quaternary eolian deposition on the Piedmont and high plains, central United States. Global and Planetary Change 11, 35–55.
Forrest, J., Clark, N.R., 1989. Characterizing grain size distributions: evaluation of a new approach using a multivariate extension of entropy analysis. Sedimentology 36, 711–722.
Friedman, G.M., 1961. Distinction between dune, beach, and river sands from their textural characteristics. Journal of Sedimentary Petrology 31, 514–529.
Friedman, G.M., 1979. Address of the retiring President of the International Association of Sedimentologists: differences in size distributions of populations of particles among sands of various origins. Sedimentology 26, 3–32.
Fryberger, S.G., Dean, G., 1979. Dune forms and wind regime. In: McKee, E. (Ed.), A Study of Global Sand Seas, U.S. Geological Survey Professional Paper 1052, pp. 137–169.
Fryberger, S.G., Ahlbrandt, T.S., Andrews, S., 1979. Origin, sedimentary features, and significance of low-angle eolian "sand sheet" deposits, Great Sand Dunes National Monument and vicinity, Colorado. Journal of Sedimentary Petrology 49, 733–746.
Galbraith, R.F., Laslett, G.M., 1993. Statistical models for mixed fission track ages. Nuclear Tracks and Radiation Measurements 21, 459–470.
Galbraith, R.F., Roberts, R.G., 2012. Statistical aspects of equivalent dose and error calculation and display in OSL dating: an overview and some recommendations. Quaternary Geochronology 11, 1–27.
Galbraith, R.F., Roberts, R.G., Laslett, G.M., Yoshida, H., Olley, J.M., 1999. Optical dating of single and multiple grains of quartz from Jinmium rock shelter, northern Australia: Part I experimental design and statistical models. Archaeometry 41, 339–364.
Gates, W.L., 1976. Modeling the ice-age climate. Science 191, 1138–1144.
Gees, R.A., 1965. Moment measures in relation to the depositional environments of sands. Eclogae Geologicae Helvetiae 58, 209–213.
Germain, D., Filion, L., 2002. Description morpho-sédimentologique d'un système éolien du haut de falaise, au Cap Sandtop à l'Île d'Anticosti (Québec). Géographie Physique et Quaternaire 56, 81–95.
Gillies, J.A., Nickling, W.G., Tilson, M., Furtak-Cole, E., 2012. Wind-formed gravel bed forms, Wright Valley, Antarctica. Journal of Geophysical Research 117, 19. F04017.
Glaister, R.P., Nelson, H.W., 1974. Grain-size distributions, an aid in facies identification. Bulletin of Canadian Petroleum Geology 22, 203–240.
Glennie, K.W., Evamy, B.D., 1968. Dikaka: plants and plant-root structures associated with aeolian sand. Palaeogeography, Palaeoclimatology, Palaeoecology 4, 77–87.
Goddard, E.N., Trask, P.D., De Ford, R.K., Rove, O.N., Singewald Jr., J.T., Overbeck, R.M., 1963. Rock-Color Chart. Geological Society of America, New York, New York.
Goman, M., Leigh, D.S., 2004. Wet early to middle Holocene conditions on the upper Coastal Plain of north Carolina, USA. Quaternary Research 61, 256–264.
Good, T.R., Bryant, I.D., 1985. Fluvio-aeolian sedimentation: an example from Banks Island, N.W.T., Canada. Geografiska Annaler. Series A, Physical Geography 67, 33–46.
Goudie, A., Watson, A., 1981. The shape of desert sand dune grains. Journal of Arid Environments 4, 185–190.
Goudie, A., Warren, A., Jones, D., Cooke, R., 1987. The character and possible origins of the aeolian sediments of the Wahiba Sand Sea, Oman. The Geographical Journal 153, 231–256.
Griffith, G.E., Omernik, J.M., Comstock, J.A., Lawrence, S., Martin, G., Goddard, A., Hulcher, V.J., Foster, T., 2001. Ecoregions of Alabama and Georgia. U.S. Geological Survey, Reston, Virginia, 1:1,700,000 scale map, 1 sheet.
Griffith, G.E., Omernik, J.M., Comstock, J.A., Schafale, M.P., McNab, W.H., Lenat, D.R., MacPherson, T.F., Glover, J.B., Shelburne, V.B., 2002. Ecoregions of North Carolina and South Carolina. U.S. Geological Survey, Reston, Virginia, 1:1,500,000 scale map, 1 sheet.
Harman, J.R., 1991. Synoptic Climatology of the Westerlies: Process and Patterns. Association of American Geographers, Washington, DC (80 pp.).
Holmes, J.A., 1893. Geology of the sand-hill country of the Carolinas. Geological Society of America Bulletin 5, 33–35.
Hsu, S.A., 1974. Computing eolian sand transport from routine weather data. In: Proceedings of the 14th Coastal Engineering Conference (24–28 June 1974), 2. Copenhagen, Denmark, pp. 1619–1626.
Ivester, A.H., Leigh, D.S., 2003. Riverine dunes on the Coastal Plain of Georgia, USA. Geomorphology 51, 289–311.
Ivester, A.H., Leigh, D.S., Godfrey-Smith, D.I., 2001. Chronology of inland eolian dunes on the coastal plain of Georgia. Quaternary Research 55, 293–302.
Ivester, A.H., Godfrey-Smith, D.I., Brooks, M.J., Taylor, B.E., 2002. Carolina Bays and inland dunes of the southern Atlantic Coastal Plain yield new evidence for regional paleoclimate. Geological Society of America, Abstracts with Programs 34 (6), 273–274.
Ivester, A.H., Godfrey-Smith, D.I., Brooks, M.J., Taylor, B.E., 2003. Concentric sand rims document the evolution of a Carolina Bay in the middle coastal plain of South Carolina. Geological Society of America, Abstracts with Programs 35 (6), 169.
Jackson, S.T., Webb, R.S., Anderson, K.H., Overpeck, J.T., Webb III, T., Williams, J.W., Hansen, B.C.S., 2000. Vegetation and environment in eastern north America during the last glacial maximum. Quaternary Science Reviews 19, 489–508.
Johnson Jr., H.S., 1961. Fall line stratigraphy northeast of Columbia, S. C. Geologic Notes [South Carolina Geological Survey] 5 (5), 81–87.
Kaczorowski, R.T., 1977. The Carolina Bays: a Comparison with Modern Oriented Lakes. University of South Carolina, Department of Geology, Coastal Research Division Technical Report No. 13-CRD (124 pp).
Katz, R.W., Parlange, M.B., Tebaldi, C., 2003. Stochastic modeling of the effects of large-scale circulation on daily weather in the southeastern U.S. Climatic Change 60, 189–216.
Kite, L.E., 1987. Cretaceous and Tertiary stratigraphy of the Gilbert 15-minute quadrangle, Lexington and Aiken Counties, South Carolina. South Carolina Geology 31, 17–27.
Kleman, J., Jansson, K., De Angelis, H., Stroeven, A.P., Hättestrand, C., Alm, G., Glasser, N., 2010. North American Ice Sheet build-up during the last glacial cycle, 115–21 kyr. Quaternary Science Reviews 29, 2036–2051.
Knight, D.B., Davis, R.E., 2007. Climatology of tropical cyclone rainfall in the southeastern United States. Physical Geography 28, 126–147.
Knight, J., Orford, J.D., Wilson, P., Wintle, A.G., Braley, S., 1998. Facies, age and controls on recent coastal sand dune evolution in north Norfolk, eastern England. Journal of Coastal Research Special issue 26, 154–161.
Kocurek, G., Nielson, J., 1986. Conditions favorable for the formation of warm-climate aeolian sand sheets. Sedimentology 33, 795–816.
Kutzbach, J.E., Guetter, P.J., Behling, P.J., Selin, R., 1993. Simulated climatic changes: results from the COHMAP climate-model experiments. In: Wright Jr., J.E., Kutzbach, J.E., Webb III, T., Ruddiman, W.F., Street-Perrott, F.A., Bartlein, P.J. (Eds.), Global Climates since the Last Glacial Maximum. University of Minnesota Press, Minneapolis, MN, pp. 24–93.
Kutzbach, J., Gallimore, R., Harrison, S., Behling, P., Selin, R., Laarif, F., 1998. Climate and biome simulations for the past 21,000 years. Quaternary Science Reviews 17, 473–506.
LaMoreaux, H.K., Brook, G.A., Knox, J.A., 2009. Late Pleistocene and Holocene environments of the southeastern United States from the stratigraphy and pollen content of a peat deposit on the Georgia Coastal Plain. Palaeogeography, Palaeoclimatology, Palaeoecology 280, 300–312.
Lancaster, N., 1986. Grain-size characteristics of linear dunes in the southwestern Kalahari. Journal of Sedimentary Petrology 56, 395–400.
Lancaster, N., 1989. The Namib Sand Sea: Dune Forms, Processes, and Sediments. A.A. Balkema, Rotterdam (200 pp.).
LeGrand, H.E., 1961. Summary of geology of Atlantic Coastal Plain. American Association of Petroleum Geologists Bulletin 45, 1557–1571.

Leigh, D.S., 1998. Evaluating artifact burial by eolian versus bioturbation processes, South Carolina Sandhills, USA. Geoarchaeology 13, 309–330.

Leigh, D.S., 2008. Late Quaternary climates and river channels of the Atlantic Coastal Plain, Southeastern USA. Geomorphology 101, 90–108.

Leigh, D.S., Feeney, T.P., 1995. Paleochannels indicating wet climate and lack of response to lower sea level, southeast Georgia. Geology 23, 687–690.

Li, C., Battisti, D.S., 2008. Reduced Atlantic storminess during last glacial maximum: evidence from a coupled climate model. Journal of Climate 21, 3561–3579.

Liu, L.Y., Skidmore, E., Hasi, E., Wagner, L., Tatarko, J., 2005. Dune sand transport as influenced by wind directions, speed and frequencies in the Ordos Plateau, China. Geomorphology 67, 283–297.

Lopez-Martinez, C., Grimalt, J.O., Hoogakker, B., Gruetzner, J., Vautravers, M.J., McCave, I.N., 2006. Abrupt wind regime changes in the north Atlantic Ocean during the past 30,000–60,000 years. Paleoceanography 21, 12. PA4215.

Mahan, S.A., Miller, D.M., Menges, C.M., Yount, J.C., 2007. Late Quaternary stratigraphy and luminescence geochronology of the northeastern Mojave Desert. Quaternary International 166, 61–78.

Markewich, H.W., Markewich, W., 1994. An Overview of Pleistocene and Holocene Inland Dunes in Georgia and the Carolinas—Morphology, Distribution, Age, and Paleoclimate. U.S. Geological Survey Bulletin 2069 (32 pp.).

Markewich, H.W., Litwin, R.J., Wysocki, D.A., Pavich, M.J., 2015. Synthesis on Quaternary aeolian research in the unglaciated eastern United States. Aeolian Research 17, 139–191.

McGee, W.J., 1890. The southern extension of the Appomattox Formation. The American Journal of Science, 3rd series 40, 15–41.

McGee, W.J., 1891. The Lafayette Formation, 12th Annual Report of the United States Geological Survey to the Secretary of the Interior 1890-'91, pp. 347–521.

McIntyre, A., Kipp, N.G., Bé, A.W.H., Crowley, T., Kellogg, T., Gardner, J.V., Prell, W., Ruddiman, W.F., 1976. Glacial North Atlantic 18,000 years ago: a CLIMAP reconstruction. In: Cline, R.M., Hays, J.D. (Eds.), Investigation of Late Quaternary Paleoceanography and Paleoclimatology. Geological Society of America Memoir 145, pp. 43–76.

McKenna Neuman, C., 1989. Kinetic energy transfer through impact and its role in entrainment by wind of particles from frozen surfaces. Sedimentology 36, 1007–1015.

McKenna Neuman, C., 1990. Observations of winter aeolian transport and niveo-aeolian deposition at Crater Lake, Pangnirtung Pass, N.W.T., Canada. Permafrost and Periglacial Processes 1, 235–247.

McKenna Neuman, C., 1993. A review of aeolian transport processes in cold environments. Progress in Physical Geography 17, 137–155.

McKenna Neuman, C., 2003. Effects of temperature and humidity upon the entrainment of sediment particles by wind. Boundary-Layer Meteorology 108, 61–89.

McKenna Neuman, C., 2004. Effects of temperature and humidity upon the transport of sedimentary particles by wind. Sedimentology 51, 1–17.

McKenna-Neuman, C., Gilbert, R., 1986. Aeolian processes and landforms in glaciofluvial environments of southeastern Baffin Island, N.W.T., Canada. In: Nickling, W.G. (Ed.), Aeolian Geomorphology. Allen and Unwin, Boston, pp. 213–235.

Mix, A.C., 1992. The marine oxygen isotope record: constraints on timing and extent of ice-growth events (120-65 ka). In: Clark, P.U., Lea, P.D. (Eds.), The Last Interglacial-Glacial Transition in North America. Geological Society of America Special Paper 270, pp. 19–30.

Moiola, R.J., Weiser, D., 1968. Textural parameters: an evaluation. Journal of Sedimentary Petrology 38, 45–53.

Moiola, R.J., Phillips, B.J., Weiser, D., 1968. Differentiation of beach, river, and inland dune sands by whole-phi textural parameters. Oklahoma Geology Notes 28, 61–64.

Moore, C.R., Brooks, M.J., Mallinson, D.J., Parham, P.R., Ivester, A.H., Feathers, J.K., 2014. Rapid scour, sand rim construction, and basin migration of a Carolina Bay in southeastern North Carolina. Geological Society of America Abstracts with Programs 46 (3), 96–97.

Moore, C.R., Brooks, M.J., Mallinson, D.J., Parham, P.R., Ivester, A.H., Feathers, J.K., 2016. The Quaternary evolution of Herndon Bay, a Carolina Bay on the Coastal Plain of North Carolina (USA): implications for paleoclimate and oriented lake genesis. Southeastern Geology 51, 145–171.

Morton, R., 1995. Soil Survey of Chesterfield County, South Carolina. U.S. Soil Conservation Service, Washington, DC (206 pp.).

Murray, A.S., Wintle, A.G., 2000. Luminescence dating of quartz using an improved single-aliquot regenerative-dose protocol. Radiation Measurements 32, 57–73.

Murray, A.S., Wintle, A.G., 2003. The single aliquot regenerative dose protocol: potential for improvements in reliability. Radiation Measurements 37, 377–381.

Murray, A.S., Marten, R., Johnston, A., Martin, P., 1987. Analysis for naturally occurring radionuclides at environmental concentrations by gamma spectrometry. Journal of Radioanalytical and Nuclear Chemistry 115, 263–288.

Nystrom Jr., P.G., Kite, L.E., 1988. The Pinehurst Formation in South Carolina. Geological Society of America, Abstracts with Programs 20 (4), 307–308.

Nystrom Jr., P.G., Willoughby, R.H., Price, L.K., 1991. Cretaceous and Tertiary stratigraphy of the Upper Coastal Plain, South Carolina. In: Horton Jr., J.W., Zullo, V.A. (Eds.), The Geology of the Carolinas. University of Tennessee Press, Knoxville, pp. 221–240.

Oglesby, R.J., Maasch, K.A., Saltzman, B., 1989. Glacial meltwater cooling of the Gulf of Mexico: GCM implications for Holocene and present-day climates. Climate Dynamics 3, 115–133.

Otto-Bliesner, B.L., Brady, E.C., Clauzet, G., Tomas, R., Levis, S., Kothavala, Z., 2006. Last glacial maximum and Holocene climate in CCSM3. Journal of Climate 19, 2526–2544.

Otwell, W.L., Johnson Jr., H.S., Heron Jr., S.D., 1966. The D. T. Duncan kaolin property, Richland and Kershaw Counties, South Carolina. Geologic Notes [South Carolina Geological Survey] 10, 9–15.

Overpeck, J.T., Webb, R.S., Webb III, T., 1992. Mapping eastern North American vegetation change of the past 18 ka: No-analogs and the future. Geology 20, 1071–1074.

Powars, D.S., 2000. The effects of the Chesapeake Bay impact crater no the geologic framework and the correlation of hydrogeologic units of southeastern Virginia, south of the James River. U.S. Geological Survey Professional Paper 1622, 53.

Powers, M.C., 1953. A new roundness scale for sedimentary particles. Journal of Sedimentary Petrology 23, 117–119.

Prescott, J.R., Hutton, J.T., 1994. Cosmic ray contributions to dose rates for luminescence and ESR dating: Large depths and long-term time variations. Radiation Measurements 23, 497–500.

Reimann, T., Lindhorst, S., Thomsen, K.J., Murray, A.S., Frechen, M., 2012. OSL dating of mixed coastal sediment (Sylt, German Bight, north Sea). Quaternary Geochronology 11, 52–67.

Reimer, P.J., Baillie, M.G.L., Bard, E., Bayliss, A., Beck, J.W., Blackwell, P.G., Bronk Ramsey, C., Buck, C.E., Burr, G.S., Edwards, R.L., Friedrich, M., Grootes, P.M., Guilderson, T.P., Hajdas, I., Heaton, T.J., Hogg, A.G., Hughen, K.A., Kaiser, K.F., Kromer, B., McCormac, F.G., Manning, S.W., Reimer, R.W., Richards, D.A., Southon, J.R., Talamo, S., Turney, C.S.M., van der Plicht, J., Weyhenmeyer, C.E., 2009. IntCal09 and Marine09 radiocarbon age calibration curves, 0–50,000 years cal BP. Radiocarbon 51, 1111–1150.

Ridgeway, D.C., McCauley, J.F., Colquhoun, D.J., 1966. Geology of the Blaney Quadrangle, South Carolina. South Carolina Geological Survey Map Series MS-11, 1: 24,000 scale, 1 sheet.

Ruz, M.-H., Allard, M., 1995. Sedimentary structures of cold-climate coastal dunes, eastern Hudson Bay, Canada. Sedimentology 42, 725–734.

Sahsamanoglou, H.S., 1990. A contribution to the study of action centres in the North Atlantic. International Journal of Climatology 10, 247–261.

Saye, S.E., Pye, K., 2006. Variations in chemical composition and particle size of dune sediments along the west coast of Jutland, Denmark. Sedimentary Geology 183, 217–242.

Selby, M.J., Rains, R.B., Palmer, R.W., 1974. Eolian deposits of the ice-free Victoria Valley, southern Victoria Land, Antarctica. New Zealand Journal of Geology and Geophysics 17, 543–562.

Shin, S.-L., Liu, Z., Otto-Bleisner, N., Brady, E.C., Kutzbach, J.E., Harrison, S.P., 2003. A simulation of the last glacial maximum climate using the NCAR-CCSM. Climate Dynamics 20, 127–151.

Shuman, B., Bartlein, P., Logar, N., Newby, P., Webb III, T., 2002. Parallel climate and vegetation responses to the early Holocene collapse of the Laurentide Ice Sheet. Quaternary Science Reviews 21, 1793–1805.

Slee, J., Uchupi, E., Trumbull, J.V.A., 1964. Statistical parameters of Cape Cod beach and eolian sands. U.S. Geological Survey Professional Paper 501-D, D118–D122.

Solohub, J.T., Klovan, J.E., 1970. Evaluation of grain-size parameters in lacustrine environments. Journal of Sedimentary Petrology 40, 81–101.

Sorrie, B.A., 2011. A Field Guide to Wildflowers of the Sandhills Region: North Carolina, South Carolina, Georgia. University of North Carolina Press, Chapel Hill, North Carolina (378 pp.).

Soulé, P.T., 1998. Some spatial aspects of southeastern United States climatology. Journal of Geography 97, 142–150.

Stahle, D.W., Cleaveland, M.K., 1992. Reconstruction and analysis of spring rainfall over the southeastern U.S. for the past 1000 years. Bulletin of the American Meteorological Society 73, 1947–1961.

Stapor, F.W., Tanner, W.F., 1975. Hydrodynamic implications of beach, beach ridge and dune grain size studies. Journal of Sedimentary Petrology 45, 926–931.

Street, F.A., Grove, A.T., 1979. Global maps of lake-level fluctuations since 30,000 yr B.P. Quaternary Research 12, 83–118.

Stuiver, M., Reimer, P., 1993. Extended 14C data base and revised CALIB 3.0 14C age calibration program. Radiocarbon 35, 215–230.

Swezey, C.S., Fitzwater, B.A., Whittecar, G.R., 2016. Geology and geomorphology of the Carolina Sandhills, Chesterfield County, South Carolina. In: Doar III, W.R. (Ed.), Gold, Structures, and Landforms in Central South Carolina – Field Guides for the GSA Southeastern Section Meeting, Columbia, South Carolina, 2016, Geological Society of America Field Guide 42, 9–36.

Swezey, C.S., Schultz, A.P., Alemán González, W., Bernhardt, C.E., Doar III, W.R., Garrity, C.P., Mahan, S.A., McGeehin, J.P., 2013. Quaternary eolian dunes in the valley of the Savannah River, Jasper County, South Carolina. Quaternary Research 80, 250–264.

Swift, D.J.P., Heron, S.D., 1969. Stratigraphy of the Carolina Cretaceous. Southeastern Geology 10, 201–245.

Taira, A., Scholle, P.A., 1979. Discrimination of depositional environments using settling tube data. Journal of Sedimentary Petrology 49, 787–800.

Taylor, B.E., Rich, F.J., Brooks, M.J., Ivester, A.H., Clement, C.O., 2011. Late Pleistocene and Holocene vegetation changes in the sandhills, Fort Jackson, South Carolina. Southeastern Geology 48, 147–163.

Thom, B.G., 1970. Carolina Bays in Horry and Marion Counties, South Carolina. Geological Society of America Bulletin 81, 783–814.

Thomas, D.S.G., 1987. Discrimination of depositional environments using sedimentary characteristics in the Mega Kalahari, central southern Africa. In:

Frostick, L., Reid, I. (Eds.), Desert Sediments: Ancient and Modern. Geological Society, London Special Publication 35, 293–306.
Thornthwaite, C.W., 1931. The climate of North America according to a new classification. Geographical Review 21, 633–655.
Thornthwaite, C.W., 1948. An approach toward a rational classification of climate. Geographical Review 38, 55–94.
Tucker, R.W., Vacher, H.L., 1980. Effectiveness of discriminating beach, dune, and river sands by moments and the cumulative weight percentages. Journal of Sedimentary Petrology 50, 165–172.
van der Plas, L., Tobi, A.C., 1965. A chart for judging the reliability of point counting results. American Journal of Science 263, 87–90.
Watts, W.A., 1980. Late-Quaternary vegetation history at White Pond on the inner Coastal Plain of South Carolina. Quaternary Research 13, 187–199.
Watts, W.A., 1983. Vegetational history of the eastern United States 25,000 to 10,000 years ago. In: Porter, S.C. (Ed.), The Late Pleistocene, Late-Quaternary Environments of the United States, vol. 1, pp. 294–310.
Webb III, T., Bartlein, P.J., Harrison, S.P., Anderson, K.H., 1993. Vegetation, lake levels, and climate in eastern North America for the past 18,000 years. In: Wright Jr., J.E., Kutzbach, J.E., Webb III, T., Ruddiman, W.F., Street-Perrott, F.A., Bartlein, P.J. (Eds.), Global Climates since the Last Glacial Maximum. University of Minnesota Press, Minneapolis, MN, pp. 415–467.
Weber, A.H., Buckley, R.L., Parker, M.J., Harvey, R.P., Hamby, D.M., 2003. The creation of an historical meteorological database for environmental dose assessment. Environmental Monitoring and Assessment 83, 255–281.
Wentworth, C.K., 1922. A scale of grade and class terms for clastic sediments. Journal of Geology 30, 377–392.
Willard, D.A., Bernhardt, C.E., Brooks, G.R., Cronin, T.M., Edgar, T., Larson, R., 2007. Deglacial climate variability in central Florida, USA. Palaeogeography, Palaeoclimatology, Palaeoecology 251, 366–382.
Whitehead, D.R., 1973. Late-Wisconsin vegetational changes in unglaciated eastern North America. Quaternary Research 3, 621–631.
Whitlock, C., Bartlein, P.J., Markgraf, V., Ashworth, A.C., 2001. The midlatitudes of north and south America during the last glacial maximum and early Holocene: similar paleoclimate sequences despite differing large-scale controls. In: Markgraf, V. (Ed.), Interhemispheric Climate Linkages. Academic Press, San Diego, pp. 391–416.
Whittecar, G.R., Fitzwater, B.A., 2016. Boundaries of soils used as contacts for eolian Pinehurst Formation, Patrick, S.C. (1:24,000) geologic map. Geological Society of America, Abstracts with Programs 48 (3). https://gsa.confex.com/gsa/2016SE/webprogram/Paper273374.html.
Willemse, N.W., Koster, E.A., Hoogakker, B., van Tatenhove, F.G.M., 2003. A continuous record of Holocene eolian activity in west Greenland. Quaternary Research 59, 322–334.
Williams, J.W., 2002. Variations in tree cover in North America since the last glacial maximum. Global and Planetary Change 35, 1–23.
Williams, J.W., Webb III, T., Richard, P.H., Newby, P., 2000. Late Quaternary biomes of Canada and the eastern United States. Journal of Biogeography 27, 585–607.
Wintle, A.G., Murray, A.S., 2006. A review of quartz optically stimulated luminescence characteristics and their relevance in single-aliquot regeneration dating protocols. Radiation Measurements 41, 369–391.
Wolfe, J.A., 1979. Temperature parameters of humid to mesic forests of eastern Asia and relation to forests of other regions of the northern hemisphere and Australasia. U.S. Geological Survey Professional Paper 1106 (37 pp.).
Woodcock, D.W., Wells, P.V., 1990. Full-glacial summer temperatures in eastern North America as inferred from Wisconsinan vegetational zonation. Palaeogeography, Palaeoclimatology, Palaeoecology 79, 305–312.